

Response to review #1

We thank the anonymous referee #1 for his/her encouraging comments and suggestions for improvements. Below, the referee comments are in green, our response in black and the changed/added sections to the manuscript in *italics*.

1) SPIN is a new instrument and I think this might be the first published ice nucleation data making use of this instrument. Hence, the paper needs to ‘validate’ the instrument as thoroughly as possible. The homogeneous freezing results for ammonium sulphate are valuable in this respect. However, this paper is about heterogeneous nucleation and I would like to see some heterogeneous results for a material which has been studied in the past and a comparison made.

In addition to homogeneous freezing of ammonium sulphate droplets, heterogeneous ice nucleation of mineral dust was investigated with SPIN, and the results were compared to literature. In particular, deposition and immersion freezing of NX-illite was investigated, with both the version of SPIN used in the present study and the final version of SPIN, and the observed ice nucleation onset conditions were found to be in good agreement with those measured by Welti et al. (2009). These results, as well as instrumental calibrations, are described in detail in a current SPIN technical paper by Garimella et al. (2016). At the time of submission of the present study, the technical paper was not yet available online and we could not cite it.

We have included the following paragraph on page P35725, line 19:

*“The final version and the performance of SPIN are described in more detail by Garimella et al. (2016). The main difference between the version of SPIN used in the present study and the final version is related to better temperature control of the final version.”*

2) P35722 In 7-8. The Kramer et al. and Cziczo et al. references are for cirrus clouds, not mixed phase clouds. There are plenty of papers out there which discuss mixed phase clouds including two relatively recent review articles:(Hoose and Möhler, 2012; Murray et al., 2012).

The referee is correct – the Krämer et al. (2009) and Cziczo et al. (2013) references are for cirrus clouds. We have modified lines 6-8 on page P35722: *“Heterogeneous ice nucleation is considered to be an important pathway for ice formation in the troposphere, especially in mixed-phase clouds (Hoose and Möhler, 2012; Murray et al., 2012), but also in cirrus clouds (Krämer et al., 2009; Cziczo et al., 2013).”*

3) P35722 In 20. The reference to Zobrist et al. in the context of ‘suggestions that these SOA particles could play a role in ice nucleation’ is incorrect. Zobrist et al. (2008) suggested the opposite – they suggested that glassy aerosol would not nucleate ice. This was one of the reasons why it was so surprising that Murray et al. (2010) showed that aqueous glassy aerosol

could nucleate ice under upper tropospheric conditions. Also, Virtanen et al. (2010) did not discuss SOA nucleating ice in any detail – it is just mentioned in the abstract.

We thank the referee for pointing out the misplacement of the citation. We have moved the references to Zobrist et al. (2008) and Virtanen et al. (2010) after the first part of the sentence and inserted a reference to Murray et al. (2010) at the end of the sentence. The sentence now reads: “*Secondary organic aerosol (SOA) can exist in a semi-solid, amorphous state in the atmosphere (Zobrist et al., 2008; Virtanen et al., 2010), and it has been suggested that amorphous SOA particles could play a role in ice nucleation (Murray et al., 2010).*”

4) P35723, In 10-13. The authors refer to modelling studies. It is important to also note the modelling studies performed by Murray et al. (2010) and also Price et al. (2015). These studies are highly relevant here.

We have added references to Murray et al. (2010) and Price et al. (2015), as well as Lienhard et al. (2015) to the text and also discuss these studies throughout the paper.

5) P35723, In 25-30. The authors suggest that the SOA in Mohler et al. (2008) liquefied and froze homogeneously. The SOA only nucleated well above water saturation. This implied that it was so hydrophobic that it did not take up water until an extreme supersaturation.

In Möhler et al. (2008) the pure  $\alpha$ -pinene SOA nucleated ice at very high ice supersaturation ( $S_{ice}=1.7$ ), but still at subsaturated conditions with respect to water. Therefore, we do not agree with the referee comment here. We have clarified the sentence on page P35723, line 26: “*Thus, it is likely that these particles never featured a high viscosity, liquefied easily and the resulting droplets froze homogeneously.*”

6) P35731, I am confused by the discussion of the dependence on size here. It seems to be stated in the text that there is no significant size dependence of ice nucleation, but when I look at fig 4 I see that there is a clear dependence on size. Bigger particles nucleate ice at a lower S.

There is no clear dependence on size. When looking at Fig. 4, it can be seen that 330 nm particles indeed nucleate ice at highest saturation ratios, but 550 nm particles nucleate ice at lower saturation ratios than 800 nm particles. Therefore it is inconclusive whether there is a size dependence or not. We have also created a supplementary Table S1 listing the ice nucleation onset conditions for 1, 5 and 10 % frozen fractions for each experiment, from which it is easy to see that no clear size dependence can be observed.

7) The authors need to discuss and use the results from Price et al. (2015) throughout their paper. In Price et al. the diffusion coefficient of water in the water soluble fraction of SOA from alpha pinene was quantified over a range of temperatures and RHs. Using these measurements the uptake of water into a solution droplet was modelled for a variety of conditions. They conclude that ‘SOM can take hours to equilibrate with water vapour under very cold conditions’ and ‘for 100 nm particles predicts that under mid- to upper-tropospheric conditions radial inhomogeneities in water content produce a low viscosity surface region and

more solid interior, with implications for heterogeneous chemistry and ice nucleation' This is highly relevant and complementary for this paper. For example, when making a judgment concerning the timescale of transformation from a glassy solid to a liquid the pertinent quantity is diffusion. The diffusion coefficient can be used to estimate this timescale. This should be done, for example, on P 35733 (ln 18-30) where the authors note that they observe ice nucleation at an RH well above the RH at which they observe these aerosol to transform to liquid aerosol.

The referee is correct in pointing out that the findings of this paper support the conclusions of Price et al. (2015). However, quantifying the diffusion coefficient of water in the alpha-pinene SOA is beyond the scope of this paper. We have added a new section 3.4 "*Freezing mechanisms*" on page P35732 where the results and implications of Price et al. (2015) are discussed. For more details, please see our response to comment #10 below.

8) P35736, ln 5-10. When commenting that biogenic SOA may be mixed with sulphates and that this may be important for ice nucleation, it would be sensible to bring in the work of Wilson et al. (2012) who showed that glassy aerosol containing a mixture of carboxylic acids and ammonium sulphate also nucleated ice.

We have added the following sentence on page 35736, line 9: "*It has already been shown that glassy aerosol containing a mixture of carboxylic acids and ammonium sulphate nucleates ice (Wilson et al., 2012).*"

9) P35736. A discussion is needed about how their fraction 'frozen' is far higher than previous investigations at the AIDA chamber (Wilson et al., 2012; Murray et al., 2010). Could this be related to the particle size? The studies at the AIDA chamber were with smaller particles than those used here.

Our study indicates that seed particle size does not seem to be an important parameter in the size range we have investigated. The substances studied by Wilson et al. (2012) and Murray et al. (2010) are not the same as what we studied, and their experimental approaches and procedures were different, so we would not necessarily expect similar frozen fractions.

We have added a paragraph on this topic to the literature comparison in section 3.5:

*"When comparing the frozen fractions of this study to earlier studies with SOA proxies, such as the substances studied by Wilson et al. (2012) and Murray et al. (2010), it is worth noting that much higher frozen fractions are achieved in this study. Most likely the difference lies in the experimental methods used: in Wilson et al. (2012) and Murray et al. (2010), the freezing was studied in an expansion chamber, not a continuous flow diffusion chamber such as SPIN. Thus, we would also not necessarily expect similar frozen fractions. "*

10) The authors use the term deposition mode. This should be caveated. Is this true deposition? i.e. deposition of ice directly onto glassy aerosol particles? Or could nucleation occur in the layer of lower viscosity solution which the modelling of Price et al. (2015) (and others) show will form when RH around glassy aerosol is increased? This layer of lower

viscosity water has also been experimentally observed in the work from Jonathan Reid's group.

We agree that the ice nucleation could occur in the liquid or lower viscosity layer on the particles rather than as direct deposition of ice onto glassy particles. We have limited the use of 'deposition mode' and replaced it with 'heterogeneous ice nucleation' in the text.

Another possible freezing mechanism could be immersion freezing of large, suspended, ice nucleating organic macromolecules formed through oligomerisation during the ageing process in the CLOUD chamber. Organic macromolecules have been suggested to be the ice nucleation active entity causing the observed immersion freezing of e.g. birch pollen washing water (Pummer et al., 2012). That could explain why we do not observe any clear particle size effect on the ice nucleation behaviour.

We have added a new section 3.4 to the text discussing possible freezing mechanisms (below). Due to partly overlapping content between sections 3.4 and 3.5, we have also shortened section 3.5 considerably.

*“The results presented in the section above clearly indicate heterogeneous freezing of SOA particles below saturation with respect to water vapour. Various freezing mechanisms could potentially be in play. It can be speculated that we observe (i) deposition nucleation occurring directly onto highly viscous SOA particles; (ii) immersion freezing of partly deliquesced SOA particles, where the core of the particle is still (highly) viscous; (iii) hygroscopic growth of the particles leading to freezing of droplets due to suspensions of large organic molecules. The relevance of the first two potential freezing processes are related to the relative timescales of the viscosity transition vs the freezing of the SOA particles for increasing humidities as discussed e.g. by Berkemeier et al. (2014), Lienhard et al. (2015) and Price et al. (2015). Lienhard et al. (2015) conclude that heterogeneous freezing of biogenic SOA particles would be highly unlikely at temperatures higher than 220 K in the atmosphere since according to their modelling, the timescales of equilibration would be very short. On the other hand, the modelling results presented by Price et al. (2015) indicate that  $\alpha$ -pinene SOA particles are likely to exhibit viscous core-liquefied shell morphologies on timescales long enough to facilitate ice nucleation via the suggested mechanism (ii) in our study.*

*In this context, it is worth mentioning that the maximum ice nucleation time in SPIN is of the order of 10 s. However, nucleation taking place on much shorter timescales can be observed if the nucleation rates are high enough to yield detectable numbers of ice crystals. In other words, the observed number of ice crystals corresponds to the time integral over the nucleation rate distribution. This implies that from our measurements, no further conclusions concerning nucleation times and rates can be drawn.*

*The (iii) potential freezing mechanism has been reported for ice nucleating macromolecules (INM) originating from pollen (Pummer et al., 2012). It is not likely that the molecules formed in the current study grow to masses comparable to the several kDa reported for the pollen macromolecules (Pummer et al., 2012), but it does not necessarily rule out that large enough molecules or agglomerates to facilitate freezing may have been produced during the conducted experiments, even though it did not seem to be the case in previous comparable studies (Möhler et al., 2008; Ladino et al., 2014). Based on the current*

*study, it is not possible to conclude which heterogeneous freezing mechanism(s) may be dominating.”*

We have also removed the words “*in the deposition mode*” from the Conclusions (P35736, line 17) and added a sentence to line 24: “*We were not able to distinguish between three possible freezing mechanisms: i) deposition nucleation onto highly viscous SOA particles; ii) immersion freezing of partly deliquesced SOA particles; or iii) hygroscopic growth and subsequent freezing of the SOA particles due to presence of organic ice nucleating macromolecules.*”

11) The data for SOA proxies from (Wilson et al., 2012; Murray et al., 2010) must be shown in Figure 6. I suggest the authors focus on the onset RHs where the aerosol was thought to start in a glassy state.

These data are now included in Fig. 6, with the following extension to the caption:

*“The red squares show the deposition ice nucleation onsets for glassy citric acid (Murray et al., 2010) and the freezing results of 4 glassy SOA proxies from (Wilson et al., 2012) are shown by blue squares (raffinose M5AS), green squares (levoglucosan), magenta squares (raffinose), and black squares (HMMA).”*

12) I note that the co-authors of the Leinhard et al. ACP 2015 paper have posted a comment, so I won't write much about this. But, I reinforce that comment and state that the Leinhard paper should be discussed in the present manuscript.

Please see our response to the open comment by Ulrich Krieger. The work by Lienhard et al. (2015) is also discussed in the new section 3.4 (for details, please see our response to comment #10 above).

## References

- Baustian, K. J. et al., Atmos. Chem. Phys., 13, 5615-5628, 2013  
Cziczo, D. J. et al, Science, 340, 1320–1324, 2013  
Garimella, S. et al., Atmos. Meas. Tech. Discuss., doi:10.5194/amt-2015-400, in review, 2016  
Hoose, C. and Möhler, O., Atmos. Chem. Phys., 12, 9817–9854, 2012  
Krämer, M. et al., Atmos. Chem. Phys., 9, 3505–3522, 2009.  
Ladino, L. et al., J. Geophys. Res.-Atmos., 9041-9051, 2014  
Lienhard, D. et al., Atmos. Chem. Phys., 13599-13613, 2015  
Möhler, O. et al., Env. Res. Lett., 3, doi:10.1088/1748-9326/3/2/025007, 2008  
Murray, B. J. et al., Nat. Geosci., 3, 233-237, 2010  
Murray, B. J. et al., Chem. Soc. Rev., 41, 6519-6554, 2012  
Price, H. et al., Chem. Sci., 6, 4876-4883, 2015  
Pummer, B. et al., Atmos. Chem. Phys., 12, 2541-2550, 2012.

Virtanen, A. et al., *Nature*, 467, 824–827, 2010  
Wang, B. et al., *J. Geophys. Res.-Atmos.*, 117, D16209, doi:10.1029/2012JD018063, 2012  
Welti, A. et al., *Atmos. Chem. Phys.*, 9, 6705-6715, 2009  
Wilson, T. et al., *Atmos. Chem. Phys.*, 12, 8611-8632, 2012  
Zobrist, B. et al., *Atmos. Chem. Phys.*, 8, 5221-5244, 2008

## Response to review #2

We thank the anonymous referee #2 for his/her comments and suggestions for improvements. Below, the referee comments are in green, our response in black and the changed/added sections to the manuscript in *italics*.

1) As the first publication for this instrument from this group, this manuscript would benefit from more detailed descriptions of instrumental calibrations; most notably missing are an explicit description of the optical particle counter (OPC) calibration as well as a description of the instrument backgrounds. While the former omission, the OPC calibration, was partially described in the experimental section, more details are needed e.g., how many sizes of glass beads and what assumptions/analysis was conducted to get the full size distributions in the upper right panels of Figures 1 and 3. As for the latter, it seems qualitatively clear that signal is above the background in the upper right panels of Figures 1 and 3, but establishing background counts will be crucial to correctly quantifying frozen fractions and outline the frozen fraction limit of detection.

Most of the details of the instrumental calibrations were omitted because there is a technical paper on SPIN by Garimella et al. (2016) currently online. At the time of submission of the present study, the technical paper was not yet available online and we could not cite it. Although the instrument we have used in this study is the version previous to the one presented in Garimella et al. (2016), the descriptions of the optics calibration as well as establishing the background counts are features that have not changed during the upgrade to the current version of SPIN.

Two sizes of polystyrene latex spheres (PSL), 0.9 and 2  $\mu\text{m}$ , and glass beads of 5 and 8  $\mu\text{m}$  were used to calibrate the optical detector of SPIN. A power law fit was applied to the calibration data in order to obtain the full size distribution. The detection efficiency of the OPC was investigated with different sizes of monodisperse PSL spheres in the range from 300 nm to 1.0  $\mu\text{m}$ . Typical backgrounds during the experiments were of the order of 10-20 particles per litre.

We have included the following paragraphs to the text:

On page P35725, line 19:

*“The final version and the performance of SPIN are described in more detail by Garimella et al. (2016). The main difference between the version of SPIN used in the present study and the final version is related to better temperature control of the final version.”*

On page P35726, line 5 we have modified the sentence *“The size measurements of the SPIN OPC were calibrated using glass beads in the size range from 0.5 to 11.4  $\mu\text{m}$ .”* to *“The size measurements of the SPIN OPC were calibrated using two sizes of polystyrene latex spheres (PSL), 0.9 and 2  $\mu\text{m}$ , and glass beads of 5 and 8  $\mu\text{m}$ .”* and added sentences *“A power law fit was applied to the calibration data and the full size distribution was extrapolated from the fit. The detection efficiency of the OPC was investigated with different sizes of monodisperse PSL spheres in the range from 300 nm to 1.0  $\mu\text{m}$ .”* and *“Typical backgrounds during the experiments were of the order of 10-20 particles per litre.”*

2) Taking a closer look at Figure 1, it looks like the transition from regime A to regime B occurs at 97% RH, which corresponds to an ice saturation ratio ( $S_{ice}$ ) of 1.38. This is lower than the value reported for homogeneous freezing, likely because the authors have chosen a 10% activated fraction as their onset conditions for homogeneous freezing of ammonium sulfate. Given the onset conditions of the  $\alpha$ -pinene SOA were at 1%, would not a 1% activated fraction for homogeneous freezing be a better comparison? This choice may have large implications for the results of the paper and should be addressed by the authors. For example, if 1% activated fraction for homogeneous freezing does indeed occur at an  $S_{ice}$  of 1.38, then those homogeneous freezing points would overlap with the points that the authors consider to be heterogeneous freezing for their viscous  $\alpha$ -pinene SOA. To add clarity to this discussion, the authors may also choose to show a frozen fraction vs.  $S_{ice}$  plot as a supplemental figure; in doing so, the authors will increase the manuscript's transparency by allowing the reader to compare the maximum activated fractions from heterogeneous nucleation to those activated fractions seen in homogeneous freezing.

We have not used the transition from regime A to regime B to obtain our ice nucleation onset T and RH. Instead, the transition from regime B to regime C is used. This is because the operation mode of the instrument version used here was limited to only heating the SPIN chamber walls or keeping one wall at constant temperature and heating the other (warm) wall. The temperature control of the colder wall during active cooling was observed to be inadequate in most cases, resulting in "cold pockets" inside the chamber. Thus, the ice nucleation "onset" here is actually "offset": we do a temperature scan with a constant wall temperature difference in order to investigate the T and RH at which the ice disappears. These conditions correspond to the ice nucleation onset conditions.

The 10% activated fraction was chosen because of better counting statistics in the case of homogeneous freezing of ammonium sulphate droplets. We have now plotted the 10% activated fractions for the  $\alpha$ -pinene SOA as well, for better comparison and consistency, and included the ice nucleation onset conditions of viscous  $\alpha$ -pinene SOA for 1, 5 and 10 % activated fractions in the supplementary Table S1.

We have added a paragraph to section 2.3 for clarification (P35728, line 15):

*"The way ice nucleation onsets in these homogeneous freezing experiments are obtained is the following. In Fig. 1, we use the transition from regime B to regime C, not from regime A to regime B, to obtain the ice nucleation onset temperature and ice saturation ratio. Due to the risk of cold pockets forming during active wall cooling, we scan the aerosol sample temperature upwards until the observed ice crystal mode vanishes and only liquid droplets remain. This temperature, at which a certain fraction (e.g. 10 %) of ice remains, is considered the ice nucleation onset. Although the ice nucleation onset here is actually ice offset, the conditions correspond to the ice nucleation onset conditions."*

We have also added another clarifying paragraph to section 2.3 (P35729, line 2):

*"It would be expected that > 10% of the droplets formed inside SPIN are exposed to temperatures > 0.3 °C below the reported average aerosol sample temperatures, which can*

*explain most of the gap between the reported average aerosol temperatures and the theoretical homogeneous freezing temperature.”*

3) The authors mention that they first show “size distributions in order to distinguish depositional nucleation from homogeneous freezing;” however, no explicit description of how the size distributions facilitate this was explained. To the reviewer, the size distribution B in both Figure 1 and 3 do look qualitatively different, but I am not sure how that correlates to depositional vs. homogeneous freezing. In the reviewer’s opinion, an explicit explanation of this differentiation and all underlying assumptions would greatly increase the clarity provide further transparency to the results section.

The referee is correct: the size distributions themselves do not give exact information about the freezing mode. We have rephrased the sentence “*First, we show size distributions in order to distinguish deposition nucleation from homogeneous freezing*” on page P35729, line 26 to “*First, we show size distributions in order to demonstrate how we distinguish between inactivated seed aerosol particles, ice crystals and liquid droplets*”.

Also, we have modified a sentence in the Conclusions (P35736, line 16): the sentence “*We conducted reproducible measurements and applied a size distribution method*” has been changed to “*We conducted reproducible measurements and performed uncertainty estimation and modelling of the temperatures and ice saturation ratios inside the INP counter*”.

4) The authors also mentioned in this section testing for “droplet breakthrough,” or that RH where a fraction of the formed liquid droplets survive the evaporation region; from size distribution C in Figure 1 it looks like droplet breakthrough may happen at relatively low supersaturations. Do the authors have any quantitative numbers for droplet breakthrough RH at the temperatures explored? Additionally, it appears from the upper right panel of Figure 3 that, when droplet breakthrough occurs (regime C), the authors also seen a large suppression of homogeneous freezing despite being at -36.8 °C and above water saturation. The reviewer suggests the authors address this behavior to increase the utility of the paper.

The droplet breakthrough for SPIN is systematically investigated and reported in Garimella et al. (2016). Following this issue raised by the referee, we have reconsidered our interpretation of what we previously considered as liquid droplets in Figure 3. It is more likely that at the temperatures investigated, the large size mode in Fig. 3 panel C consists of frozen droplets that have not grown very much due to potential activation close to the evaporation section of SPIN. This would also explain the slightly higher S/P ratios compared to Fig. 1 panel C.

We have removed the sentence on page P35730 lines 9-11 “*The latter experiment was performed in order to investigate droplet breakthrough, i.e. at which RH a fraction of the formed liquid droplets remain as droplets after the SPIN evaporation section.*” since droplet formation, not droplet breakthrough, was investigated in the experiment. We have also removed the last sentence of the paragraph (P35730, lines 15-17) and replaced it with “*The droplet mode in panel (c) likely consists of frozen droplets that have not grown very much due to potential activation close to the evaporation section of SPIN. This could also explain the slightly higher S/P ratios (0.3) compared to the S/P ratios of 0.1–0.2 for the liquid droplets in Fig. 1 (c).*”

It is not clear which freezing mechanism is responsible for the freezing we observe in Fig. 3 regime C. It does take place at conditions where we have observed homogeneous freezing of highly diluted ammonium sulphate droplets, but we cannot distinguish whether it is caused by homogeneous freezing of liquefied SOA, immersion freezing of partly deliquesced SOA with a highly viscous core, or immersion freezing of droplets containing suspensions of organic ice nucleating macromolecules such as reported by Pummer et al. (2012). Therefore, we refrain from using the term “homogeneous freezing” in this context. The possible different freezing mechanisms are discussed in a new added section 3.4 (P35732). For details, please see below.

5) The error bars here are represented by the statistical standard deviation ( $1.96\sigma$ ) between measured points. While the reviewer appreciates the authors providing this metric as it indicates that the ice nucleation onsets are reproducible between experiments and/or the aerosol is physio-chemically similar between experiments, the reviewer would argue that this does not necessarily conclude that these points are statistically different from homogeneous nucleation. The authors are comparing experimentally derived ice nucleation points to water saturation derived from a parameterization. This analysis ignores the instrumental uncertainties associated with the SPIN. The authors mention throughout the text the temperature uncertainty ( $\pm 0.4$  K); however an associated RH/ $S_{ice}$  error has not been explicitly addressed for the heterogeneous nucleation points. Interestingly, the authors did provide a maximum  $S_{ice}$  error for the  $\alpha$ -pinene SOA homogeneous freezing point and it was  $+0.13/-0.11$ . Similar-sized instrumental uncertainties for the heterogeneous freezing regime would clearly put at least 1% of the aerosol into homogeneous freezing conditions. The authors should explain, in detail, how their instrumental uncertainties factor into how they differentiate homogeneous and heterogeneous freezing.

We thank the referee for useful suggestions for improving the uncertainty estimation of our results. Consequently, we have re-evaluated our data and applied a more suitable way of representing the instrumental uncertainties of the observed ice nucleation onset temperature and  $S_{ice}$ .

The temperatures of the SPIN chamber walls were monitored with 4 pairs of thermocouples on each side, and the aerosol lamina temperature and  $S_{ice}$  are corrected for the buoyancy effect following Rogers (1988) at each of the 4 locations. The deviation in the temperatures vertically along the walls needs to be taken into account when estimating the uncertainties in the ice saturation ratio  $S_{ice}$ .

We have used the random instrumental error in average aerosol sample temperature from our measurements of homogeneous freezing with ammonium sulphate also in the case of SOA particles. This instrumental error is the standard deviation of  $0.50^\circ\text{C}$  from the reproducible temperature measurements of homogeneous freezing. The mentioned  $\pm 0.4$   $^\circ\text{C}$  range is related to the modelled temperature range to which the aerosol sample was exposed to during the homogeneous freezing experiments where the temperature difference between the walls was pronounced.

In order to obtain meaningful estimates for uncertainties in  $S_{ice}$ , we take the modelled equilibrium maximum range the aerosol sample is possibly exposed to, based on the pairwise temperature readings of the chamber walls. The modelled maximum range in sample

temperature and saturation ratio is illustrated in supplementary Fig. S1. If the maximum saturation ratio with respect to water the sample is exposed to is under the homogeneous freezing line (Koop et al., 2000) or the water saturation line, freezing is considered heterogeneous. This is the basis for our differentiation between homogeneous and heterogeneous freezing.

We have now plotted the 10 % activated fractions of the SOA particles in Fig. 5 in order to allow for better comparison with homogeneous freezing of ammonium sulphate droplets. 10 % frozen fraction was not reached in every experiment; thus, the number of data points in Fig. 5 has decreased. Also, re-evaluation of the data has revealed such large uncertainties in  $S_{ice}$  for some data points that they may be susceptible to large systematic errors, and it is no longer possible to determine at which conditions the freezing was initiated. Such data points have also been omitted.

We have added the following paragraph to the manuscript:

P35729, line 23:

*“The standard deviation of the experimentally determined homogeneous freezing temperatures for 10 % frozen fractions is 0.50 °C. This variation can be considered to reflect the experimental random errors on the average aerosol sample temperature for the instrument for these operation conditions.”*

We have re-written section 3.3 in the following way (P35731):

*“The ice nucleation onset conditions were systematically investigated for frozen fractions of 1, 5 and 10 %. These data are listed in Table S1. In general, the conditions for the observations of 1, 5 and 10 % frozen fractions were very similar. In Fig. 5 the conditions for 10% frozen fractions are depicted. The random instrumental error on the average aerosol sample temperature is expected to be similar to the variations observed above for homogeneous freezing with a standard deviation of 0.5 °C. The depicted range of the saturation ratio with respect to ice ( $S_{ice}$ ) is the modelled equilibrium maximum range the aerosol sample possibly is exposed to - in the vertical and horizontal dimensions - based on the pairwise temperature readings of the chamber walls at 4 locations. This is illustrated in Fig. S1. The modelling is done by taking the warm and cold wall temperature pairs at the 4 thermocouple locations where they are monitored and then calculating the aerosol lamina temperatures and saturation ratios with respect water and ice at those locations according to Rogers (1988). The reported ice nucleation onset temperatures in Fig. 5 are the mean values of the 4 aerosol lamina temperatures, and the reported  $S_{ice}$  values are the mean values of the 4 calculated lamina  $S_{ice}$  values. All the maximum saturation ratios for the observed 10% frozen fractions are below the depicted lines in Fig. 5 indicating where homogeneous freezing occurs. In terms of the saturation ratio with respect to water, the maximum modelled values are found in the range 0.90-0.98 and in the range 0.92-0.98 for frozen fractions of 1 and 10%, respectively. For the water saturation to reach 1 for all of these freezing conditions, a systematic wall temperature deviation in between thermocouples of >2 °C would be required. Such a systematic wall temperature deviation is highly unlikely considering the reasonable and reproducible homogeneous freezing results presented above. Hence, it is highly unlikely*

*that the observed freezing occurring at subsaturated conditions with respect to water is homogeneous freezing.*

*From our measurements, we have a strong indication that the studied  $\alpha$ -pinene SOA induced ice nucleation heterogeneously. Despite instrumental limitations, the results were reproducible and the uncertainty for the ice nucleation onset temperatures and supersaturations could be inferred."*

Page 35721, line 18: Delete "(IN)," this abbreviation is unnecessary here

Done.

Page 35722, line 2: Delete "e.g.," this is unnecessary here

Done.

Page 35722, line 5: Change "and contributes" to "and can contribute"

Done.

Page 35722, line 7: Given the references, did the authors mean "cold-cloud" instead of "mixed-phase cloud?"

Yes. This change has been made to the text on lines 6-8 on page P35722: "*Heterogeneous ice nucleation is considered to be an important pathway for ice formation in the troposphere, especially in mixed-phase clouds (Hoose and Möhler, 2012; Murray et al., 2012), but also in cirrus clouds (Krämer et al., 2009; Cziczo et al., 2013).*"

Page 35724, line 26: Please give a brief description of why aspherical here means viscous as this does not make sense out of context of (Järvinen et al., 2015)

The assumption of asphericity being indicative of high viscosity for SOA particles is the result of investigations of the optical properties of SOA formed and exposed to different temperatures and humidities. During the experiments, the near-backscattering depolarisation ratio measured by the SIMONE-Junior instrument was used to detect the phase of the particles. Liquid particles have a spherical shape and do not change the polarisation state of the incident light. Viscous phase state can change the particle morphology so that a non-zero depolarisation ratio is observed. Here, a non-zero depolarisation ratio was measured throughout the growth of the SOA particles at low RH, which indicated a viscous phase state. (Järvinen et al., 2016)

The lines 24-26 on page P35724 "*The depolarisation ratio was measured, and based on the determined depolarisation of the incident light, it was determined that the particles were aspherical and thus viscous.*" have been modified to: "*The depolarisation ratio was measured, and based on the determined depolarisation ratio of the backscattered light, it was determined whether the particles were aspherical and thus viscous (detectable depolarisation).*" Also, for clarity and consistency, line 29 on page P35724 has been modified to "*the phase transition of the particles from higher to lower viscosity or liquid phase, i.e. the point where the depolarisation ratio decreased significantly to a level of spherical particles.*"

Page 35725, line 3: If 80% RH is the transition RHw for this  $\alpha$ -pinene SOA, the authors may consider to re-define their freezing mode as immersion-mode freezing as per (Berkemeier et al., 2014)

The referee is correct: the freezing mode is not necessarily pure deposition nucleation, but immersion freezing of the liquid/low  $\eta$ -viscosity outer layer of the SOA particles, following the suggested ‘core-shell-morphologies’ in Berkemeier et al. (2014) and more recently in Price et al. (2015).

Another possibility could be immersion freezing of large, suspended organic macromolecules formed through oligomerisation during the ageing process in the CLOUD chamber. Organic macromolecules have been suggested to be the ice nucleation active entity causing the observed immersion freezing of e.g. birch pollen washing water (Pummer et al., 2012). That could explain why we do not observe any clear particle size effect on the ice nucleation behaviour.

We have added a new section 3.4 to the text (below). Due to partly overlapping content between sections 3.4 and 3.5, we have also shortened section 3.5 considerably.

*“The results presented in the section above clearly indicate heterogeneous freezing of SOA particles below saturation with respect to water vapour. Various freezing mechanisms could potentially be in play. It can be speculated that we observe (i) deposition nucleation occurring directly onto highly viscous SOA particles; (ii) immersion freezing of partly deliquesced SOA particles, where the core of the particle is still (highly) viscous; (iii) hygroscopic growth of the particles leading to freezing of droplets due to suspensions of large organic molecules. The relevance of the first two potential freezing processes are related to the relative timescales of the viscosity transition vs the freezing of the SOA particles for increasing humidities as discussed e.g. by Berkemeier et al. (2014), Lienhard et al. (2015) and Price et al. (2015). Lienhard et al. (2015) conclude that heterogeneous freezing of biogenic SOA particles would be highly unlikely at temperatures higher than 220 K in the atmosphere since according to their modelling, the timescales of equilibration would be very short. On the other hand, the modelling results presented by Price et al. (2015) indicate that  $\alpha$ -pinene SOA particles are likely to exhibit viscous core-liquified shell morphologies on timescales long enough to facilitate ice nucleation via the suggested mechanism (ii) in our study.*

*In this context, it is worth mentioning that the maximum ice nucleation time in SPIN is of the order of 10 s. However, nucleation taking place on much shorter timescales can be observed if the nucleation rates are high enough to yield detectable numbers of ice crystals. In other words, the observed number of ice crystals corresponds to the time integral over the nucleation rate distribution. This implies that from our measurements, no further conclusions concerning nucleation times and rates can be drawn.*

*The (iii) potential freezing mechanism has been reported for ice nucleating macromolecules (INM) originating from pollen (Pummer et al., 2012). It is not likely that the molecules formed in the current study grow to masses comparable to the several kDa reported for the pollen macromolecules (Pummer et al., 2012), but it does not necessarily rule out that large enough molecules or agglomerates to facilitate freezing may have been produced during the conducted experiments, even though it did not seem to be the case in*

*previous comparable studies (Möhler et al., 2008; Ladino et al., 2014). Based on the current study, it is not possible to conclude which heterogeneous freezing mechanism(s) may be dominating.”*

Page 35726, line 29: If the absolute concentration is always under 1000 cm<sup>-3</sup>, what is the frozen fraction limit of detection?

The lower limit of the frozen fraction to be determined depends on the investigated particle number concentration and the observed background – which both varied between different experiments. However, typically the lower limit for most experiments would be at the order of 1x10<sup>-4</sup>. We have added a sentence to page P35726, line 29: *“The frozen fraction lower limit of detection was typically of the order of 1x10<sup>-4</sup>.”*

Page 35729, line 9: While interesting, I am not sure why the authors report the freezing depression for 200 nm particles as 500 nm particles were used in this study

Also 200 nm particles were used in the measurements, as mentioned in the text on page 35727, line 10. The example in Fig. 1 is from an experiment with 500 nm particles.

Page 35730, line 6: Change “Analogously” to “Analogous” – Done.

## References

- Berkemeier, T., et al., Atmos. Chem. Phys., 14, 12513-12531, 2014  
Garimella, S. et al., Atmos. Meas. Tech. Discuss., doi:10.5194/amt-2015-400, in review, 2016  
Järvinen, E. et al., Atmos. Chem. Phys., 16, 3651-3664, 2016  
Koop, T. et al., Nature, 406, 611-614, 2000  
Ladino, L. et al., J. Geophys. Res.-Atmos., 9041-9051, 2014  
Lienhard, D. et al., Atmos. Chem. Phys., 13599-13613, 2015  
Möhler, O. et al., Env. Res. Lett., 3, doi:10.1088/1748-9326/3/2/025007, 2008  
Price, H. et al., Chem. Sci., 6, 4876-4883, 2015  
Pummer, B. et al., Atmos. Chem. Phys., 12, 2541-2550, 2012.  
Rogers, D., Atmos. Res., 22, 149-181, 1988.

## Reply to the Interactive Comment by Ulrich Krieger

We thank U. Krieger and his co-authors for the short comment concerning discussion of the timescales of equilibration and their effects on the ice nucleation potential of  $\alpha$ -pinene SOA in our paper. In the revised version of the paper, we extend the discussion of the topic to include the recent studies by Lienhard et al. (2015) and Price et al. (2015). Below we reply to the concerns raised in the short comment.

We would first like to clarify why we believe that we observe heterogeneous ice nucleation. Based on instrument validation studies considering the homogeneous freezing of highly diluted ammonium sulphate droplets, as shown in Fig. 1 and 2 in the paper, we obtain the random instrumental uncertainty in temperature with a standard deviation of 0.5 K. We have modelled (according to Rogers (1988)) the equilibrium maximum range in the ice saturation ratio the aerosol sample possibly is exposed to - in the vertical and horizontal dimensions - based on the temperature readings of the chamber walls. For consistency, we have plotted 10 % frozen fractions for the SOA particles in Fig. 5. All the maximum saturation ratios for the observed 10 % frozen fractions are below the depicted lines in Fig. 5 indicating where homogeneous freezing occurs. In terms of the saturation ratio with respect to water, the maximum modelled values are found in the range 0.90-0.98 and in the range 0.92-0.98 for frozen fractions of 1 and 10 % respectively. For the water saturation to reach 1 for all of these freezing conditions - a systematic wall temperature deviation of  $> 2$  K in between the thermocouples would be required. Such a systematic wall temperature deviation is highly unlikely considering the reasonable and reproducible homogeneous freezing results presented in the paper. Hence, it is highly unlikely that the observed freezing occurring at subsaturated conditions with respect to water can be considered homogeneous freezing.

Therefore, we interpret the ice nucleation as being heterogeneous. We agree that it is possible that the heterogeneous ice nucleation we observe could be immersion freezing of partly deliquesced SOA particles having “core-shell morphology”, as suggested by Berkemeier et al. (2014) and Price et al. (2015), instead of “pure” deposition nucleation of water vapour onto insoluble ice nucleating particles. This and other possible freezing mechanisms are discussed in detail in the revised version of the paper.

The SOA measured in this study was the same as in Järvinen et al. (2015), and the observed transition from aspherical to spherical form, interpreted as a change in viscosity from semi-solid to liquid, happened at approximately  $RH = 80$  % at  $T = 235$  K. Thus, at  $RH > 80$  % the SOA would be liquid in an equilibrium state. It was also observed by Järvinen et al. (2015) that the phase transition was not instantaneous, but the transition timescales from semi-solid to liquid were of the order of minutes. In order for heterogeneous ice nucleation to occur at  $RH = 93$  % before liquefaction of the SOA, we agree that the nucleation rate needs to be sufficiently fast, and this is possible with SPIN. The nucleation times in SPIN can be of the order of tenths of seconds or even shorter.

Here, we would like to correct a misconception in the short comment: the nucleation time of a few seconds reported by Welti et al. (2012) with the ice nucleation chamber ZINC, an instrument somewhat similar to SPIN, is the residence time inside the instrument and only represents the maximum time available for ice nucleation. Actual nucleation times can be significantly shorter, and some of the particles may nucleate ice even instantaneously after entering the SPIN chamber.

In Lienhard et al. (2015), the  $\alpha$ -pinene SOA particles were produced in a flow tube reactor at room temperature and collected onto filters, after which they were extracted and the water-soluble part of the SOA was studied as single particles levitated in electrodynamic balance to determine the diffusion coefficients of water in the SOA. The diffusion coefficients of water in  $\alpha$ -pinene SOA at lower temperatures ( $T = 249.5$  K and lower) were measured only up to water activities of 0.5 due to instrumental limitations. A Vignes-type parameterisation derived from model substances was applied and fitted to the SOA data, with predictions of high diffusion coefficients at the upper end of the water activity spectrum. Based on these fits and parcel model simulations it was concluded that atmospheric SOA particles are most likely in equilibrium with the surrounding relative humidity, thus making heterogeneous ice nucleation on these particles unlikely to occur above 220 K.

In the present study, we observe heterogeneous ice nucleation in the upper end of the water activity spectrum at 235 K. While the model fits shown in Fig. 2 in Lienhard et al. (2015) agree well with the measurements in the case of SOA proxies such as levoglucosan and sucrose, for  $\alpha$ -pinene SOA the actual measurement points at  $T=249.5$  K,  $T=232$  K and  $T=209.5$  K at measured water activity range ( $a_w < 0.5$ ) do not indicate a clear increase in the diffusion coefficients and the agreement with the measurements and parametrization is not as obvious as for the proxies. At higher water activities where the Vignes-type parametrization shows a drastic increase in diffusion coefficient values there are no data points. The fact that the parametrizations presented in the Lienhard et al. (2015) do not agree with the ice nucleation measurement data presented in our work – provided that the freezing we observe is either deposition nucleation on highly viscous SOA or immersion freezing of partly deliquesced SOA - brings up interesting questions and should be a topic of future studies. Interestingly, our results support the simulation results of Price et al. (2015) who suggest that core-shell morphologies could exist at moderate to high updraft speeds at 230 K and lower temperatures.

Another aspect to consider is that in our study, the SOA particles were slightly less oxidised ( $O:C = 0.25$ ). Furthermore, we did the measurements using online methods, not the water extract of the SOA filter samples. Hence, the composition of the SOA particles in our study may differ significantly from that used in Lienhard et al. (2015), which could affect the properties controlling the water uptake and ice nucleation of these SOA particles.

Finally, we fully agree that the competition between liquefaction of the particle by water uptake and its ability to trigger heterogeneous ice nucleation is of crucial importance. Nevertheless, we would like to stress that much is still unknown of this topic, and as there is possibly such a significant and important difference in the atmospheric implications between

the results of our paper and that of Lienhard et al. (2015), we think it is absolutely crucial that future experimental and modelling studies address this topic.

## References

- Berkemeier, T. et al., *Atmos. Chem. Phys.*, 14, 12513–12531, 2014.  
Järvinen, E. et al., *Atmos. Chem. Phys.*, 16, 3651-3664, 2016.  
Lienhard, D. M. et al., *Atmos. Chem. Phys.*, 15, 3599–13613, 2015.  
Price, H. C. et al., *Chem. Sci.*, 6, 4876-4883, 2015.  
Rogers, D., *Atmos. Res.*, 22, 149-181, 1988.  
Welti, A. et al., *Atmos. Chem. Phys.*, 12, 9893-9907, 2012.

# Heterogeneous ice nucleation of viscous secondary organic aerosol produced from ozonolysis of $\alpha$ -pinene

**K. Ignatius<sup>1</sup>, T. B. Kristensen<sup>1</sup>, E. Järvinen<sup>2</sup>, L. Nichman<sup>3</sup>, C. Fuchs<sup>4</sup>, H. Gordon<sup>5</sup>, P. Herenz<sup>1</sup>, C. R. Hoyle<sup>4,6</sup>, J. Duplissy<sup>7</sup>, S. Garimella<sup>8</sup>, A. Dias<sup>5</sup>, C. Frege<sup>4</sup>, N. Höppel<sup>2</sup>, J. Tröstl<sup>4</sup>, R. Wagner<sup>7</sup>, C. Yan<sup>7</sup>, A. Amorim<sup>9</sup>, U. Baltensperger<sup>4</sup>, J. Curtius<sup>10</sup>, N. M. Donahue<sup>11</sup>, M. W. Gallagher<sup>3</sup>, J. Kirkby<sup>5,10</sup>, M. Kulmala<sup>7</sup>, O. Möhler<sup>2</sup>, H. Saathoff<sup>2</sup>, M. Schnaiter<sup>2</sup>, A. Tomé<sup>12</sup>, A. Virtanen<sup>13</sup>, D. Worsnop<sup>14</sup>, and F. Stratmann<sup>1</sup>**

<sup>1</sup>Leibniz Institute for Tropospheric Research (TROPOS), 04318 Leipzig, Germany

<sup>2</sup>Institute of Meteorology and Climate Research – Atmospheric Aerosol Research, Karlsruhe Institute of Technology, Karlsruhe, Germany

<sup>3</sup>School of Earth, Atmospheric and Environmental Sciences, University of Manchester, Manchester, M13 9PL, UK

<sup>4</sup>Laboratory of Atmospheric Chemistry, Paul Scherrer Institute, Villigen, Switzerland

<sup>5</sup>CERN, 1211 Geneva, Switzerland

<sup>6</sup>WSL Institute for Snow and Avalanche Research SLF Davos, Switzerland

<sup>7</sup>Department of Physics, P.O. Box 64, 00014 University of Helsinki, Finland

<sup>8</sup>Massachusetts Institute of Technology, Cambridge, MA, USA

<sup>9</sup>SIM/CENTRA and F. Ciências, Universidade de Lisboa, Lisboa, Portugal

<sup>10</sup>Goethe-University of Frankfurt, Institute for Atmospheric and Environmental Sciences, Altenhöferallee 1, 60438 Frankfurt am Main, Germany

<sup>11</sup>Center for Atmospheric Particle Studies, Carnegie Mellon University, Pittsburgh, PA 15213, USA

<sup>12</sup>SIM/IDL, Universidade da Beira Interior, Covilhã, Portugal

<sup>13</sup>Department of Applied Physics, University of Eastern Finland, Kuopio, Finland

<sup>14</sup>Aerodyne Research, Inc., Billerica, MA 08121, USA

Correspondence to: K. Ignatius (ignatius@tropos.de)

## Abstract

There are strong indications that particles containing secondary organic aerosol (SOA) exhibit amorphous solid or semi-solid phase states in the atmosphere. This may facilitate ~~deposition~~-heterogeneous ice nucleation and thus influence ~~cirrus~~ cloud properties. However, experimental ice nucleation studies of biogenic SOA are scarce. Here, we investigated the ice nucleation ability of viscous SOA particles.

The SOA particles were produced from the ozone initiated oxidation of  $\alpha$ -pinene in an aerosol chamber at temperatures in the range from  $-38$  to  $-10$  °C at 5–15 % relative humidity with respect to water to ensure their formation in a highly viscous phase state, i.e. semi-solid or glassy. The ice nucleation ability of SOA particles with different sizes was investigated with a new continuous flow diffusion chamber. For the first time, we observed heterogeneous ice nucleation of viscous  $\alpha$ -pinene SOA ~~in the deposition mode~~ for ice saturation ratios between 1.3 and 1.4 significantly below the homogeneous freezing limit. The maximum frozen fractions found at temperatures between  ~~$-36.5$~~ - $-39.0$  and  ~~$-38.3$~~ - $-37.2$  °C ranged from 6 to 20 % and did not depend on the particle surface area. Global modelling of monoterpene SOA particles suggests that viscous biogenic SOA particles are indeed present in regions where cirrus cloud formation takes place. Hence, they could make up an important contribution to the global ice ~~nuclei (IN)~~-nucleating particle budget.

## 1 Introduction

Atmospheric aerosol particles are known to influence the Earth's radiative balance and climate directly by reflecting and absorbing sunlight, and indirectly through their influence on clouds, e.g. when the particles act as cloud condensation nuclei (CCN) and/or ice ~~nuclei~~ (~~IN~~nucleating particles (INPs)) (Yu et al., 2006). Determining the role of aerosols in ice nucleation is particularly complex because of different pathways through which ice forms in the atmosphere. Ice nucleation can be either homogeneous – freezing of pure water or solute droplets – or heterogeneous, in which case ice formation is induced by foreign sur-

faces such as ~~e.g.~~ mineral dust or bacteria (Pruppacher and Klett, 1997). Homogeneous ice nucleation requires temperatures below approximately  $-37^{\circ}\text{C}$  and high supersaturations, typically ice saturation ratios  $S_{\text{ice}}$  of 1.4 or larger (Koop et al., 2000), and ~~contributes can contribute~~ to cirrus cloud formation.

Heterogeneous ice nucleation is considered to be an important pathway for ice formation in the troposphere, especially in mixed-phase clouds (~~Hoose and Möhler, 2012; Murray et al., 2012), but also in cirrus clouds~~ (Krämer et al., 2009; Cziczo et al., 2013). Immersion freezing of aerosol particles activated into supercooled cloud droplets is the most important process for primary ice formation down to temperatures of around  $-35^{\circ}\text{C}$ . Deposition ice nucleation, on the other hand, is more relevant at lower temperatures, and the typical ~~IN-INPs~~ inducing deposition nucleation are different mineral dusts, such as clay minerals and Saharan dust (DeMott et al., 2003; Möhler et al., 2006; Welti et al., 2009; Hoose and Möhler, 2012). DeMott et al. (2010) found that only about 1 in  $10^5$  or  $10^6$  atmospheric aerosol particles can act as an ~~ININP~~. In heterogeneous ice nucleation, the surface area of the seed particles typically plays an important role ~~so that the~~, ~~so that~~ larger particles tend to be more efficient ~~IN-INPs~~ (Connolly et al., 2009; Welti et al., 2009).

Secondary organic aerosol (SOA) can exist in a semi-solid, amorphous state in the atmosphere (~~Zobrist et al., 2008; Virtanen et al., 2010~~), and it has been suggested that ~~these amorphous~~ SOA particles could play a role in ice nucleation (~~Zobrist et al., 2008; Virtanen et al., 2010~~) (~~Murray et al., 2010~~). SOA is produced in the atmosphere from oxidation and subsequent condensation of volatile organic compounds (VOCs) (Hallquist et al., 2009) of which the majority are biogenic (Guenther et al., 1995; Jimenez et al., 2009). SOA is very abundant especially in the lower troposphere where it comprises around 30 to 70 % of the submicron particulate mass (Kanakidou et al., 2005). Monoterpenes such as  $\alpha$ -pinene are one of the most common biogenic SOA precursors, especially in boreal forest regions (Laaksonen et al., 2008). Other precursors include e.g. limonene in Australian Eucalyptus forests (Suni et al., 2007) and isoprene (Guenther et al., 2006).

The phase state of SOA depends on temperature and relative humidity (RH) (Zobrist et al., 2008) and has recently received more attention, since it determines the impact of SOA on cloud formation and therefore climate (Renbaum-Wolff et al., 2013). Depending on particle hygroscopicity, the viscosity of SOA is RH dependent; e.g. SOA produced from ozonolysis of  $\alpha$ -pinene is known to take up water at high relative humidities (Pajunoja et al., 2015). Since humidity conditions vary significantly in the troposphere, SOA particles may exhibit many different phase states during their lifetime in the atmosphere. Ice particle residuals from cirrus clouds sampled in situ were rich in oxidized organic matter (Froyd et al., 2009, 2010), which indicates that viscous or glassy organic particles may also have acted as ~~IN-INPs~~ during cirrus formation. Modelling studies suggest that viscous SOA could be an important ~~IN-INP~~ especially at low temperatures and low humidities, i.e. in the cirrus regime (~~Koop et al., 2011; Adler et al., 2013; Berkemeier et al., 2014~~)(~~Murray et al., 2010; Koop et al., 2010~~). Furthermore, experimental studies of the ice nucleation ability of viscous SOA proxies support the model findings. In chamber expansion studies, ~~glassy~~ citric acid, raffinose and levoglucosan particles nucleated ice heterogeneously at temperatures between ~~-50-80~~ and ~~-80~~<sup>50</sup> °C (Murray et al., 2010; Wagner et al., 2012; Wilson et al., 2012). Sucrose, glucose and citric acid particles were found to be very efficient ~~INs-INPs~~ in the deposition mode at temperatures between -70 and -40 °C since they nucleated ice at low ice saturation ratios ( $S_{ice} = 1.1$ ) (Baustian et al., 2013). Simulated SOA from aqueous phase reactions of methylglyoxal and methylamine have also shown ice nucleation potential in the deposition mode (Schill et al., 2014).

Amorphous SOA particles generated via gas-phase oxidation of naphthalene with OH radicals are considered relatively efficient ~~IN-INPs~~ (Wang et al., 2012). Ladino et al. (2014) and Möhler et al. (2008) reported SOA produced from ozonolysis of  $\alpha$ -pinene to be a poor or inefficient ~~IN-INP~~. In both studies, however, the phase state of SOA particles was not investigated experimentally, and the particles were produced at room temperature in a separate aerosol preparation chamber from which a fraction of them was transferred to the actual ice nucleation chamber. Thus, it is likely that ~~the particles had such a low viscosity that they liquified before freezing~~ ~~these particles never featured a high viscosity, liquefied easily~~

[and the resulting droplets froze](#) homogeneously. Ladino et al. (2014) also pointed out that precooling of the  $\alpha$ -pinene SOA particles made them slightly better [ININPs](#), possibly due to a change in viscosity.

Here, we report first observations of [deposition-heterogeneous](#) ice nucleation of laboratory generated viscous, semi-solid  $\alpha$ -pinene SOA. The phase state of the SOA particles was detected via the depolarisation signal of light scattered from the particles, using a novel optical method described in detail in a companion study (Järvinen et al., 2016). A new portable [IN-INP](#) counter was used to sample the SOA particles and measure their ice nucleation efficiency. Finally, a global model was applied to investigate to what extent viscous SOA particles could contribute to the global [IN-INP](#) budget.

## 2 Methods

### 2.1 Experimental setup: chamber experiments

The SOA particles were produced in the CLOUD (Cosmics Leaving Outdoor Droplets) chamber at CERN ([Duplissy et al., 2010, 2016; Kirkby et al., 2011](#)) ([Duplissy et al., 2010, 2016](#)) during the CLOUD9 campaign between 25 October and 3 November 2014. SOA particles were produced from ozonolysis of  $\alpha$ -pinene at low relative humidity with respect to water ( $RH_w$ ) (5–15 %) at 4 different temperatures,  $-10$ ,  $-20$ ,  $-30$  and  $-38$  °C, which are relevant for the free troposphere.  $\alpha$ -pinene and ozone were introduced to the chamber at the rate of 10 and 1000 mL min<sup>-1</sup> (respectively) over a time period of a few minutes. UV lights (Philips TUV 130 W XPT lamp) were on during this time, resulting in the photolysis of O<sub>3</sub> and OH formation. High number concentrations of particles ( $> 10^5$  cm<sup>-3</sup>) quickly formed a monomodal size distribution which grew to approximately 100 nm in diameter. During the particle growth,  $\alpha$ -pinene and ozone were continually introduced into the chamber. The particles were grown to approximately 600–800 nm in diameter in order to follow the size-dependence of their optical properties. The depolarisation ratio was measured, and based on the determined depolarisation of the [incident-backscattered](#) light, it was

determined ~~that whether~~ the particles were aspherical and thus ~~viscous~~(~~highly~~) ~~viscous~~ (~~detectable depolarisation~~). Then the  $RH_w$  was slowly increased for the optical detection of the phase transition of the particles from ~~viscous to liquid at~~ ~~higher to lower viscosity or liquid phase, i.e.~~ the point where the depolarisation ratio decreased ~~significantly to a level of spherical particles~~. The transition  $RH_w$  increased with the decreasing temperature, from 35 % at  $-10^\circ\text{C}$  to 80 % at  $-38^\circ\text{C}$ . Further experimental details are explained in Järvinen et al. (2016). The ice nucleation ability of the SOA particles was measured by sampling them from the CLOUD chamber at different growth stages in order to examine particles with different sizes. In Table 1 the particle ~~size and~~ ~~sizes and number~~ concentrations for the different experiments are included together with information about the chamber temperature and humidity conditions. The particle number size distributions were measured with several Scanning Mobility Particle Sizer (SMPS) systems (20–800 nm), and optically with an Ultra High Sensitivity Aerosol Spectrometer (UHSAS, Droplet Measurement Technologies, Inc.) in the range from 60 nm to 1  $\mu\text{m}$ . In addition, an Aerodyne high-resolution time-of-flight aerosol mass spectrometer (HR-ToF AMS) was used to determine the chemical composition of the SOA particles.

## 2.2 Ice nucleation instrumentation

We used the Spectrometer for Ice Nuclei (SPIN) to measure the ice nucleation efficiency of the SOA particles generated in the CLOUD chamber. SPIN is a new, commercially available portable ~~IN-INP~~ counter manufactured by Droplet Measurement Technologies, Inc. ~~It is~~ ~~The final version and the performance of SPIN are described in more detail by Garimella et al. (2016). The main difference between the version of SPIN used in this study and the final version is related to better temperature control of the final version.~~

~~SPIN is~~ a continuous flow diffusion chamber with parallel plate geometry adapted from the design of the Portable Ice Nucleation Chamber PINC (Chou et al., 2011) and the Zurich Ice Nucleation Chamber ZINC (Stetzer et al., 2008). The aerosol sample flow ~~was is~~ set to  $1\text{ L min}^{-1}$  surrounded by a sheath flow of  $10\text{ L min}^{-1}$  ~~flowing~~ through a chamber where a supersaturation of water vapour with respect to ice is obtained by keeping two ice covered

walls at different temperatures below 0 °C. The residence time in the upper part of the chamber where ice nucleation may take place is ~~then~~ approximately 10 s. The aerosol sample ~~is and sheath air flows are~~ then exposed to an isothermal, separately temperature-controlled evaporation section where the unfrozen droplets evaporate while the ice particles are retained, prior to particle detection with a linear polarisation optical particle counter (OPC). The OPC laser is polarised, and the intensity of the backscattered light perpendicular to the incident polarisation and the intensity of ~~the~~ backscattered polarised light are measured on a particle by particle basis. The polarisation-equivalent ratio between the two intensities provides information about the phase state of the particles. The size measurements of the SPIN OPC were calibrated using ~~glass beads in the size range from 0.5 to 11.4~~ two sizes of polystyrene latex spheres (PSL), 0.9 and 2 µm, and glass beads of 5 and 8 µm. A power law fit was applied to the calibration data, and the full size distribution was extrapolated from the fit. The detection efficiency of the OPC was investigated with different sizes of monodisperse PSL spheres in the range from 300 nm to 1.0 µm. The lower detection limit of the SPIN OPC was approximately 400 nm, with a detection efficiency of ~ 50 %. For particles larger than 700 nm, the detection efficiency was close to 100 %. For particle sizes between 550 and 600 nm, the detection efficiency was approximately 80 %. This allows the SPIN OPC to detect also the seed aerosol particles if they are large enough. Typical backgrounds during the experiments with viscous SOA particles were of the order of 10-20 particles per litre. The frozen fraction lower limit of detection was typically of the order of  $1 \times 10^{-4}$ .

The temperature of the aerosol sample flow and the supersaturation with respect to ice are modelled based on the continuous measurement of the wall temperatures. Due to a temperature gradient between the walls, there is a buoyancy effect to the air mass inside the chamber, pushing the sample flow closer to the colder wall. This effect has been taken into account in the 1-D-modelling and calculations of ~~the~~ sample temperature and humidity which are done according to Rogers (1988). A Condensation Particle Counter (CPC-3720, TSI) was run parallel to SPIN during half of the runs, when the sample particle size was smaller than 500 nm. ~~Due to limitations in the cooling system and temperature control of~~

~~SPIN, the regime of operation for the current study was limited to a minimum temperature of  $-43$  for the colder wall. SPIN was~~ SPIN was operated by keeping the colder wall at constant temperature at its lower limit and ramping up the temperature of the warm wall, thus raising the sample temperature from approximately  $-40$ – $43$  to  $-35$  °C and ice saturation ratio  $S_{ice}$  from 1 to approximately 1.45–1.5 inside the instrument. In order to minimize fluctuations of the wall temperatures, the regime of operation for the current study was limited to a minimum temperature of  $-43$  °C for the colder wall.

SPIN sampled the SOA particles from the CLOUD chamber through a 1.5 m long, quarter inch stainless steel tubing, in which the residence time was approximately 2 s. As the concentrations of the SOA particles in the CLOUD chamber typically exceeded  $10\,000\text{ cm}^{-3}$ , a dilution system partly filtering away aerosol particles was used to dilute the sample so that the particle number concentrations entering SPIN would stay under  $1000\text{ cm}^{-3}$  in order to avoid saturating the optical detector. The stainless steel tubing together with the dilution system was insulated, but the temperature of the sample was not continually measured at the SPIN inlet, and it is possible that the temperature in the sampling tube was higher than in the CLOUD chamber.

### 2.3 Instrument performance ~~validation~~ evaluation by homogeneous freezing of highly diluted ammonium sulphate droplets

Homogeneous freezing of highly diluted ammonium sulphate droplets was used to ~~validate~~ evaluate the performance of the SPIN chamber and the optical detector. Ammonium sulphate particles were generated from a 1.0 mass % solution with a medical nebulizer, dried in a diffusion dryer and then size-selected by a Differential Mobility Analyser (DMA). Mean mobility diameters of 200 and 500 nm were chosen, and a CPC (CPC-3010, TSI) was run in parallel to measure the total particle concentration.

The freezing experiments were designed in the following way: first a supersaturation with respect to ice and water was created inside SPIN by diverging the wall temperatures in order to obtain the necessary temperature gradient, while keeping the sample temperature below  $-37$  °C, which is the upper threshold temperature for homogeneous freezing in the

atmosphere (Pruppacher and Klett, 1997). After water (super)saturation was achieved and ice formation observed, both walls were heated at the same rate in order to ~~the~~ increase the sample temperature but keep the water supersaturation, leading to the disappearance of ice. The temperature of the evaporation section walls was kept constant at  $-35^{\circ}\text{C}$ .

An example of such an experiment is displayed in Fig. 1. In the upper left panel, the SPIN wall and sample (lamina) temperatures, as well as the relative humidity with respect to liquid water are plotted as a function of time. The upper right panel shows the particle number concentrations in different size bins from the same experiment. At subsaturated conditions with respect to liquid water only the 500 nm seed aerosol particles are observed. When water saturation is reached shortly after 14.3 h, most of the seeds activate to droplets which then freeze, forming a distinct mode with sizes around  $5\ \mu\text{m}$ . As the sample temperature is increased, the ice mode vanishes at approximately 14.4 h and a mode consisting of liquid droplets with sizes of  $\sim 2\text{--}3\ \mu\text{m}$  remains.

In the lower three panels of Fig. 1, the ~~raw size distributions~~ size distributions measured by the SPIN OPC from the same experiment ~~corresponding to each observed mode~~ are shown. Panel (a) shows the dry 500 nm seed aerosol particles that have not yet activated. Panel (b) illustrates the situation when most of the ammonium sulphate particles have activated into droplets and frozen. Panel (c) depicts the seed aerosol and liquid, highly diluted ammonium sulphate droplets at water supersaturation at temperatures above the homogeneous freezing point. All the data are normalised with respect to total particle counts from the OPC. The polarisation-equivalent ratios ( $S/P$  ratios) from the OPC are also different for ice crystals and liquid droplets: for ice,  $S/P$  ratios vary between 0.5 and 0.6, whereas for liquid droplets the ratios are significantly smaller, between 0.1 and 0.2. This further confirms that the distinct modes in the size distributions correspond to different phase states, and the size distributions can also be used to define ice nucleation onset points.

The ~~homogeneous freezing way ice nucleation onsets in these homogeneous freezing experiments are obtained~~ is the following. In Fig. 1, we use the transition from regime B to regime C, not from regime A to regime B, to obtain the ice nucleation onset temperature and ice saturation ratio. ~~Due to the risk of cold pockets forming during active wall cooling, we~~

scan the aerosol sample temperature upwards until the observed ice crystal mode vanishes and only liquid droplets remain. This temperature, at which a certain fraction (e.g. 10 %) of ice remains, is considered the ice nucleation onset. Although the ice nucleation onset here is actually ice offset, the conditions correspond to the ice nucleation onset conditions.

The homogeneous freezing temperatures for a frozen fraction of 10 % are shown in Fig. 2. The homogeneous freezing temperatures are all found in the range from  $-37.9$  to  $-36.6$  °C, with an average value of  $-37.3$  °C. The variation in  $S_{ice}$  ~~comes~~ results from using slightly different temperature gradients to introduce a supersaturation with respect to water inside SPIN. Based on classical nucleation theory and the parameterisation of homogeneous nucleation rates of water presented by Ickes et al. (2015), a frozen fraction of 10 % can be expected for a temperature in the range from about  $-38.2$  to  $-37.6$  °C. Uncertainties and variations in the residence time and the sizes of droplets formed inside SPIN ~~results~~ result in the uncertainty in the expected homogeneous freezing temperature. Hence, the homogeneous freezing temperatures reported in Fig. 2 are within the range or slightly higher than what could be expected from theory. However, with a temperature difference between the SPIN chamber walls close to 20 °C, according to model simulations, the aerosol sample temperature range is approximately  $\pm 0.4$  °C with respect to the average temperatures presented in Fig. 2. Roughly half of the droplets formed inside SPIN will thus be exposed to temperatures down to  $\sim 0.4$  °C below the average aerosol sample temperature. It would be expected that >10% of the droplets formed inside SPIN are exposed to temperatures >0.3 °C below the reported average aerosol sample temperatures, which can explain most of the gap between the reported average aerosol temperatures and the theoretical homogeneous freezing temperature.

The freezing point depression caused by ammonium sulphate in the water droplets was calculated using the following formula:

$$\Delta T = iM \times 1.86, \quad (1)$$

where  $i$  is the van't Hoff factor of the solute,  $M$  is the molar concentration of the solution, and  $1.86 \text{ KM}^{-1}$  is the freezing point depression for an ideal solution (Seinfeld and Pandis,

2006). For ammonium sulphate,  $i = 2.04$  (Wu et al., 2011). The droplet diameter here was estimated to be  $3 \mu\text{m}$ . For 200 nm ammonium sulphate particles, this solute effect is negligible ( $\Delta T = 0.015^\circ\text{C}$ ); for 500 nm particles the freezing point depression is  $0.24^\circ\text{C}$ , which is still within the uncertainty range of the aerosol sample temperature inside SPIN. Thus, we can conclude that the droplets were dilute enough so that the presence of ammonium sulphate did not significantly influence the freezing temperature.

With all the uncertainties considered, the correspondence between theory and experimentally obtained homogeneous freezing temperatures with SPIN is good, with a systematic tendency of the experimental average aerosol temperatures being slightly too high ( $\lesssim 0.5^\circ\text{C}$ ). This off-set is likely to be due to occasional locally slightly colder chamber wall sections in between thermocouples relative to the temperature set-points. Based on the results presented in Fig. 2 it can be concluded that the aerosol sample conditions inside SPIN can be reproduced with a high-good accuracy between different experiments, and the inferred aerosol sample conditions correspond well to what can be expected from theory. The standard deviation of the experimentally determined homogeneous freezing temperatures for 10% frozen fractions is  $0.50^\circ\text{C}$ . This variation can be considered to reflect the experimental random errors on the average aerosol sample temperature for the instrument for these operation conditions.

### 3 Results and discussion

Here, we present results from deposition-heterogeneous ice nucleation measurements, on viscous  $\alpha$ -pinene SOA, obtained with SPIN. First, we show size distributions in order to distinguish deposition-nucleation from homogeneous-freezing demonstrate how we distinguish between unactivated seed aerosol, ice crystals and liquid droplets. Then, frozen fractions and ice activation conditions are presented, as well as a followed by a discussion about the possible freezing mechanisms and a comparison to literature data. Atmospheric implications of the results will be discussed in the end of the section.

### 3.1 Size distributions

Figure 3 shows results of a typical ~~deposition-ice-nucleation-ramp~~ heterogeneous ice nucleation experiment with viscous SOA particles; this example is from 26 October 2014. ~~Analogously~~ Analogous to Fig. 1, the middle three panels show two particle number size distributions observed during ~~the deposition-ice-nucleation-ramp~~ subsaturated conditions with respect to liquid water, and a size distribution from an experiment, when the RH with respect to liquid water was greater than 100 %. The ~~latter experiment was performed in order to investigate droplet breakthrough, i.e. at which RH a fraction of the formed liquid droplets remain as droplets after the SPIN evaporation section.~~ The leftmost panel (a) shows the 550 nm seed aerosol and the middle panel (b) depicts the seeds and ice (a size mode around 5  $\mu\text{m}$ ) at water subsaturated conditions. A prominent liquid droplet mode can be seen in the third panel (c), when the  $\text{RH}_w$  was greater than 100 % ~~and part of the liquified particles froze homogeneously. Also here, there was a clear difference in the polarisation equivalent,~~ and it is possible that the SOA particles liquefied and froze homogeneously, as we have observed homogeneous freezing of diluted ammonium sulphate droplets at similar conditions. The different possible freezing mechanisms will be discussed in section 3.4. The droplet mode in panel (c) likely consists of frozen droplets that have not grown very much due to potential activation close to the evaporation section of SPIN. This could also explain the slightly higher  $S/P$  ratios ~~between the liquid droplets and ice, as can be seen from the bottom three panels.~~ (0.3) compared to the  $S/P$  ratios of 0.1–0.2 for the liquid droplets in Fig. 1 (c).

### 3.2 Frozen fractions

The fraction of particles activated as ice crystals was defined as the number of particles larger than the minimum between the seed aerosol and ice crystal modes, or between the liquid droplet and ice modes, divided by the total number of particles. In the case of SOA particles, this threshold size was 3  $\mu\text{m}$ . It cannot be ruled out, however, that there is some size overlap between ice crystals and liquid droplets, since due to the design of SPIN, not

all particles nucleate ice at the same time and not all the droplets necessarily evaporate in the evaporation section.

We investigated different SOA particle sizes from 120 nm to approximately 800 nm (see Table 1 for details). Figure 4 shows exemplary frozen fractions of 330, 550 and 800 nm viscous SOA particles as a function of the ice saturation ratio. The 330 nm particles were produced in the CLOUD chamber at  $-38^{\circ}\text{C}$ , and at the time of ice formation the temperature inside SPIN was  $-37.7 \pm 0.4^{\circ}\text{C}$ – $-38.5 \pm 0.5^{\circ}\text{C}$ . The 550 nm particles were produced at  $-20^{\circ}\text{C}$ , and nucleated ice at  $-38.1 \pm 0.4^{\circ}\text{C}$ – $-37.2 \pm 0.5^{\circ}\text{C}$ ; the 800 nm particles produced at  $-10^{\circ}\text{C}$  nucleated ice at  $-37.0 \pm 0.4^{\circ}\text{C}$ – $-38.2 \pm 0.5^{\circ}\text{C}$ . The maximum frozen fractions observed were  $\sim 6$ – $20\%$  but they did not show any clear dependency on the seed particle size; nor did the 1 or 10 % ice activation onset values, although there is some variation among the different particle sizes. [This can also be seen from Table S1 which details all the ice nucleation onset conditions from each experiment day.](#)

SOA particle properties relevant for ice nucleation could depend on the chemical composition and morphology, which could depend on the chamber conditions. The mean atomic oxygen to carbon ratio (O : C) of the SOA particles inferred from AMS measurements was 0.25 throughout the different stages of the different experiments (Järvinen et al., 2016): this would suggest possibly similar chemical composition of the particles throughout the experiments. The apparent similarity in the chemical composition for different SOA particle sizes does not explain why there is no significant change in the frozen fraction or freezing onsets when the seed particles grow larger. Surface area dependency has previously been shown for deposition ice nucleation of different mineral dusts by Welti et al. (2009), but there is no indication of such a dependency for the viscous SOA particles studied here.

### 3.3 Ice nucleation onset conditions for viscous SOA

~~The ice nucleation onset conditions were defined as the temperature and ice saturation ratio when the activated (frozen) fraction of SOA particles was systematically investigated for frozen fractions of 1, 5 and 10 %. Figure 5 shows the ice nucleation onsets for viscous  $\alpha$ -pinene SOA in the deposition and homogeneous freezing mode. The error bars of~~

the deposition nucleation data are calculated from the statistical standard deviation  $\sigma$ , and represent the 95. These data are listed in Table S1. In general, the conditions for the observations of 1, 5 and 10% confidence interval ( $1.96\sigma$ ) in both temperature and supersaturation. An estimate for the instrumental temperature uncertainty was  $\pm 1^\circ\text{C}$  on both walls inside the chamber; the statistical approach gives 1.07 frozen fractions were very similar. In Fig. 5 the conditions for 10% frozen fractions are depicted. The random instrumental error on the average aerosol sample temperature is expected to be similar to the variations observed above for homogeneous freezing with a standard deviation of  $0.5^\circ\text{C}$  as the error bar for temperature, which indicates that the conservative error estimate would also have been valid. Homogeneous freezing onset was observed only once, hence the error bars in supersaturation correspond to the theoretical maximum error calculated from the estimated instrumental temperature uncertainty. The uncertainty distribution of a theoretical maximum error is, however, unknown, and cannot be treated e. g. as Gaussian or evenly distributed.

Based on investigations of size distributions and the corresponding sample temperatures and humidities for several different experiments. The depicted range of the saturation ratio with respect to ice ( $S_{ice}$ ) is the modelled equilibrium maximum range the aerosol sample possibly is exposed to - in the vertical and horizontal dimensions - based on the pairwise temperature readings of the chamber walls at 4 locations. This is illustrated in Fig. S1. The modelling is done by taking the warm and cold wall temperature pairs at the 4 thermocouple locations where they are monitored and then calculating the aerosol lamina temperatures and saturation ratios with respect water and ice at those locations according to Rogers (1988). The reported ice nucleation onset temperatures in Fig. 5 are the mean values of the 4 aerosol lamina temperatures, and the reported  $S_{ice}$  values are the mean values of the 4 calculated lamina  $S_{ice}$  values. All the maximum saturation ratios for the observed 10% frozen fractions are below the depicted lines in Fig. 5 indicating where homogeneous freezing occurs. In terms of the saturation ratio with respect to water, the maximum modelled values are found in the range 0.90-0.98 and in the range 0.92-0.98 for frozen fractions of 1 and 10%, respectively. For the water saturation to reach

1 for all of these freezing conditions, a systematic wall temperature deviation in between thermocouples of  $>2^{\circ}\text{C}$  would be required. Such a systematic wall temperature deviation is highly unlikely considering the reasonable and reproducible homogeneous freezing results presented above. Hence, it is qualitatively quite clear highly unlikely that the observed freezing facilitated by the viscous SOA particles occurs as deposition freezing occurring at sub-saturated conditions with respect to liquid water. However, water is homogeneous freezing.

From our measurements, we have a strong indication that the studied  $\alpha$ -pinene SOA induced ice nucleation heterogeneously. Despite instrumental limitations, the results were reproducible and the uncertainty for the ice nucleation onset temperatures and supersaturations could be inferred.

### 3.4 Freezing mechanisms

The results presented in the results were also analysed with statistical tools in order to test if the freezing occurred at subsaturated conditions section above clearly indicate heterogeneous freezing of SOA particles below saturation with respect to liquid water. A paired  $t$  test (assuming a Gaussian distribution of the data) showed that the difference in saturation ratio between the data points and the saturation line with respect to liquid water is statistically significant ( $p = 10^{-6}$ ). In a similar fashion the more robust Wilcoxon signed-rank test (?) confirmed a statistically significant difference ( $p = 0.003$ ).

With the size distribution method presented here, we are able to distinguish heterogeneous ice nucleation from homogeneous freezing. From our measurements, we have strong evidence that highly viscous water vapour. Various freezing mechanisms could potentially be in play. It can be speculated that we observe (i) deposition nucleation occurring directly onto highly viscous SOA particles; (ii) immersion freezing of partly deliquesced SOA particles, where the core of the particle is still (highly) viscous; (iii) hygroscopic growth of the particles leading to freezing of droplets due to suspensions of large organic molecules. The relevance of the first two potential freezing processes are related to the relative timescales of the

viscosity transition vs the freezing of the SOA particles for increasing humidities as discussed e.g. by Berkemeier et al. (2014), Lienhard et al. (2015) and Price et al. (2015). Lienhard et al. (2015) conclude that heterogeneous freezing of biogenic SOA particles would be highly unlikely at temperatures higher than 220 K in the atmosphere since according to their modelling, the timescales of equilibration would be very short. On the other hand, the modelling results presented by Price et al. (2015) indicate that  $\alpha$ -pinene SOA induces ice nucleation in the deposition mode. Despite instrumental limitations, the results were reproducible and the uncertainty for the ice nucleation onset temperatures and supersaturations could be inferred. Particles are likely to exhibit viscous core-liquified shell morphologies on timescales long enough to facilitate ice nucleation via the suggested mechanism (ii) in our study.

In this context, it is worth mentioning that the maximum ice nucleation time in SPIN is of the order of 10 s. However, nucleation taking place on much shorter timescales can be observed if the nucleation rates are high enough to yield detectable numbers of ice crystals. In other words, the observed number of ice crystals corresponds to the time integral over the nucleation rate distribution. This implies that from our measurements, no further conclusions concerning nucleation times and rates can be drawn.

The (iii) potential freezing mechanism has been reported for ice nucleating macromolecules (INM) originating from pollen (Pummer et al., 2012). It is not likely that the molecules formed in the current study grow to masses comparable to the several kDa reported for the pollen macromolecules (Pummer et al., 2012), but it does not necessarily rule out that large enough molecules or agglomerates to facilitate freezing may have been produced during the conducted experiments, even though it did not seem to be the case in previous comparable studies (Möhler et al., 2008; Ladino et al., 2014). Based on the current study, it is not possible to conclude which heterogeneous freezing mechanism(s) may be dominating.

### 3.5 Comparison to literature data

Figure 6 shows our results together with selected literature data. The ice saturation ratios we have observed for the ice nucleation onset temperatures for viscous  $\alpha$ -pinene SOA are qualitatively comparable with ice nucleation data from other SOA or SOA proxies, but the lack of data points at lower temperatures makes quantitative comparison challenging. There is notable difference between our results and those reported by Ladino et al. (2014) and Möhler et al. (2008), who found  $\alpha$ -pinene SOA to be a poor IN. In Ladino et al. (2014), the SOA particles were produced in a smog chamber and a flow tube at room temperature and then either sampled directly, or collected on teflon filters and extracted in a solution, from which the particles were formed with an atomizer and dried prior to sampling. There was no significant difference in the ice nucleation behaviour between the freshly sampled particles and filter samples. INP nucleating ice homogeneously. However, Ladino et al. (2014) also found, however, that pre-cooling of the particles made them better IN slightly better INPs, and interpret it as a result of a transition to a more viscous state, although the phase state of the particles was not studied experimentally. Thus, it is likely that the non-pre-cooled fresh particles and filter samples had a low viscosity and liquefied before ice activation in the ice nucleation chamber. In Möhler et al. (2008), the SOA particles were produced in a separate aerosol preparation chamber at room temperature, from which they were transferred to the cloud expansion chamber where they were exposed to  $\text{RH}_w > 50$  at  $-68$  before the experiments. Also here, the viscosity of the SOA particles was not investigated, and the particles did not nucleate ice in the deposition mode, but homogeneously, requiring high ice supersaturations.

In our case, the  $\alpha$ -pinene SOA were freshly generated at subzero temperatures (from  $-10$  to  $-38$ ) and low  $\text{RH}_w$  (5–15), under conditions typical for upper troposphere, and sampled directly from the CLOUD chamber. In the companion study by Järvinen et al. (2016) it was experimentally observed that for these  $\alpha$ -pinene SOA particles the transition timescales were of the order of tens of minutes. At  $-38$  the transition happened around  $\text{RH}_w = 80$ ; inside SPIN, the conditions at which deposition ice nucleation

onset was observed were between  $RH_w = 91$  and  $RH_w = 97$ . The deliquescence process from highly viscous semi-solid to liquid is not instantaneous, and depending on the temperature and the O:C ratio, the particles may persist in a viscous state over long time periods, even of the order of days (Berkemeier et al., 2014). Since the total residence time in the sampling tube and SPIN was approximately 12, it is likely that these SOA particles kept their highly viscous state even at higher humidities than the transition RH long enough to act as IN in the deposition mode. When comparing the frozen fractions of this study to earlier studies with SOA proxies, such as the substances studied by Wilson et al. (2012) and Murray et al. (2010), it is worth noting that much higher frozen fractions are achieved in this study. Most likely the difference lies in the experimental methods used: in Wilson et al. (2012) and Murray et al. (2010), the freezing was studied in an expansion chamber, not a continuous flow diffusion chamber such as SPIN. Thus, we would also not necessarily expect similar frozen fractions

When compared to other ~~IN~~INPs, such as different mineral dusts, viscous  $\alpha$ -pinene SOA requires higher ice saturation ratios for ~~+10~~% activated fraction than e.g. kaolinite and illite at  $-35$  and  $-40$  °C (Welti et al., 2009). The maximum ice fractions, on the other hand, are of the same order of magnitude. The viscous SOA particles seem to be more efficient ~~deposition mode IN~~INPs than volcanic ash at  $-35$  and  $-40$  °C measured by Hoyle et al. (2011), with similar or lower ice saturation ratios needed for ~~+10~~% activation and higher maximum ice fractions.

### 3.6 Atmospheric implications

Viscous pinene SOA particles have already been observed in the lower troposphere in field measurements in the boreal forest (Virtanen et al., 2010). The global aerosol model GLOMAP-mode (GLObal Model of Aerosol Processes) (Mann et al., 2010) was used to investigate whether to what extent viscous biogenic monoterpene SOA is likely to be present in the atmosphere. The model version used is identical to that in Riccobono et al. (2014). GLOMAP is an extension to the TOMCAT chemical transport model (Chipperfield, 2006). It includes representations of particle formation, growth via coagulation, conden-

sation and cloud processing, wet and dry deposition and in/below cloud scavenging. The horizontal resolution is  $2.8^\circ \times 2.8^\circ$  and there are 31 vertical sigma-pressure levels extending from ground level to 10 hPa. Formation of secondary particles in the model is based on CLOUD measurements of ternary  $\text{H}_2\text{SO}_4$ -organic- $\text{H}_2\text{O}$  nucleation detailed in Riccobono et al. (2014) and on a parameterisation of binary  $\text{H}_2\text{SO}_4$ - $\text{H}_2\text{O}$  nucleation (Kulmala et al., 1998). Particles grow by irreversible condensation of monoterpene oxidation products and sulphuric acid. Monoterpene emissions in the model are taken from the Guenther et al. (1995) database. The monoterpenes are oxidised with OH,  $\text{O}_3$  and  $\text{NO}_3$  assuming the reaction rates of  $\alpha$ -pinene. A fixed 13 % of the oxidation products, referred to as SORG, condenses irreversibly onto aerosol particles at the kinetic limit.

Figure 7 shows the mean annual average concentrations of SORG in parts per trillion with respect to mass (pptm). SORG represents oxidised monoterpenes and can in this respect be considered a proxy of monoterpene SOA particles. The hatched areas mark the zones in the atmosphere where the SOA particles are likely to exist in a highly viscous or even glassy phase state according to the generic estimate of SOA glass transition temperature as a function of relative humidity given by Koop et al. (2011). This parameterisation agrees with the viscosity transitions of the investigated  $\alpha$ -pinene SOA particles that were measured in the CLOUD chamber simultaneously with the ice nucleation experiments (Järvinen et al., 2016; Nichman et al., 2016). ~~At the lowest temperature ( $-38$ ) the transition RH was observed to be even slightly higher (80) than predicted by Koop et al. (2011), indicating that at low temperatures the Koop et al. (2011) generic SOA glass transition temperature model may underestimate the number of viscous SOA particles (Järvinen et al., 2016).~~

The modelled monoterpene SOA proxy concentrations are highest over land and especially in the tropics, but near the equator the conditions for particles containing monoterpene SOA to be highly viscous require higher altitudes ( $\sim 7$  km) and colder temperatures (see Fig. 7 right panel). On the other hand, strong convective updrafts may play a role carrying the SOA particles even into the tropical tropopause layer (TTL) in short enough timescales for the particles to remain highly viscous ([Berkemeier et al., 2014](#)) ([Berkemeier et al., 2014](#); [Price et al., 2015](#)), or SOA may form in

convective outflow regions, after the transport of precursor gases from lower altitudes in the troposphere. Boreal forests are a significant source of monoterpenes in spring and summer-time of the Northern Hemisphere, and model calculations displayed in Fig. 7 indicate that sufficient concentrations of viscous monoterpene SOA could exist in the upper troposphere in this region, thus being a potential source of **ice-nuclei-INPs** for cirrus cloud formation. [This is relevant assuming that the freezing mechanism is deposition nucleation of highly viscous SOA or immersion freezing of partly deliquesced SOA with a highly viscous core.](#) It should be noted that [also](#) particles with other types of SOA than  $\alpha$ -pinene SOA may facilitate ice nucleation in cirrus clouds, or persist in a viscous state at higher temperatures or humidities (Berkemeier et al., 2014). The model results presented here nevertheless indicate qualitatively that significant concentrations of SOA-forming vapours are likely to exist in parts of the troposphere where the particles they form would be in a sufficiently viscous state to act as [IN-INPs depositionally or via immersion freezing. On the other hand, if the freezing is initiated by organic INM suspended in droplets, high viscosity might not be a prerequisite for biogenic SOA to act as an INP.](#)

So far, SOA has not been considered in climate models involving ice nucleation, and it is still very challenging to quantify the actual effect, but given the potentially high ice nucleation efficiency (up to 20 % frozen fractions),  $\alpha$ -pinene and other monoterpene SOA could contribute significantly to the global **IN-INP** budget. It is likely that a significant portion of biogenic SOA in the atmosphere form mixtures with sulphates or primary particles such as mineral dusts; that will most likely also affect the ice nucleation efficiency considerably. [It has already been shown that glassy aerosol containing a mixture of carboxylic acids and ammonium sulphate nucleates ice \(Wilson et al., 2012\).](#)

## 4 Conclusions

In this study, we produced viscous  $\alpha$ -pinene SOA particles at 10 % RH at 4 different atmospherically relevant subzero temperatures,  $-10$ ,  $-20$ ,  $-30$  and  $-38$  °C, and measured their ice nucleation capability with a new portable **IN-INP** counter. We have, for the first

time, found a strong indication that ~~viscous~~-SOA produced from ozonolysis of  $\alpha$ -pinene efficiently nucleates ice. We conducted reproducible measurements and ~~applied a size distribution method~~ performed uncertainty estimation and modelling of the temperatures and ice saturation ratios inside the INP counter to determine that the ice nucleation was heterogeneous ~~and in the deposition mode. Homogeneous freezing was also observed when the conditions inside the portable IN chamber were at or above water saturation.~~ We investigated SOA particles with mean diameters from 120 to 800 nm, and no dependency was observed between the particle size and the frozen fraction/freezing onset. The frozen fractions reached a maximum of  $\sim 6$ – $20$  %. Ice saturation ratios for the observed ice nucleation onset temperatures are in line with previous literature data, but the range of observed ice nucleation onset temperatures was narrow due to instrumental limitations. ~~Therefore~~ We were not able to distinguish between three possible freezing mechanisms: i) deposition nucleation onto highly viscous SOA particles; ii) immersion freezing of partly deliquesced SOA particles; or iii) hygroscopic growth and subsequent freezing of the SOA particles due to presence of organic ice nucleating macromolecules. ~~Therefore,~~ further experimental studies are recommended.

To date, ~~viscous or glassy~~ biogenic SOA has not been considered as ~~IN~~ an INP in any climate models. Here, results from a global aerosol model suggest that  $\alpha$ -pinene SOA may exist at least regionally in considerable numbers in the upper troposphere in the cirrus regime where they would be highly viscous or glassy, which is relevant for the freezing mechanisms (i) and (ii) above. Thus boreal forests and other regions emitting monoterpenes could potentially be a significant source of ~~IN-INPs~~ IN-INPs contributing to the global ~~IN-INP~~ IN-INP budget. In order to better quantify the impact of ~~highly viscous or glassy~~ biogenic SOA as ~~IN~~ an INP to the climate, extensive future experimental and modelling studies will be needed.

*Acknowledgements.* We would like to thank Luis Ladino, Kelly Baustian, Daniel Knopf ~~and Bingbing Wang~~, Bingbing Wang and Theo Wilson for providing the data for comparison and useful discussions. We also thank CERN CLOUD technical staff and all the ITN students for their help and support, and Dan Cziczo and Thomas Conrath for assistance in SPIN development. This research has received funding from the EC seventh Framework Programme (Marie Curie Initial Training Networks MC-ITN CLOUD-TRAIN grant no. 316662), the German Federal Ministry of Education and Research

(BMBF) through the CLOUD-12 project (no. 01LK1222B), the Swiss National Science Foundation SNSF (grant no. 200021 140663), from NordForsk through the Nordic Centre of Excellence CRAICC (Cryosphere-Atmosphere Interactions in a Changing Arctic Climate), the US National Science Foundation (grants AGS1439551, AGS1447056), the Academy of Finland (decision no. 259005) and the European Research Council (ERC Starting Grant 335478).

## References

- Adler, G., Koop, T., Haspel, C., Taraniuk, I., Moise, T., Koren, I., Heiblum, R. H., and Rudich, Y.: Formation of highly porous aerosol particles by atmospheric freeze-drying in ice clouds, *P. Natl. Acad. Sci. USA*, 110, 20414–20419, 2013.
- Baustian, K. J., Wise, M. E., Jensen, E. J., Schill, G. P., Freedman, M. A., and Tolbert, M. A.: State transformations and ice nucleation in amorphous (semi-)solid organic aerosol, *Atmos. Chem. Phys.*, 13, 5615–5628, doi:10.5194/acp-13-5615-2013, 2013.
- Berkemeier, T., Shiraiwa, M., Pöschl, U., and Koop, T.: Competition between water uptake and ice nucleation by glassy organic aerosol particles, *Atmos. Chem. Phys.*, 14, 12513–12531, doi:10.5194/acp-14-12513-2014, 2014.
- Chipperfield, M. P.: New version of the TOMCAT/SLIMCAT off-line chemical transport model: intercomparison of stratospheric tracer experiments, *Q. J. Roy. Meteorol. Soc.*, 132, 1179–1203, 2006.
- Chou, C., Stetzer, O., Weingartner, E., Jurányi, Z., Kanji, Z. A., and Lohmann, U.: Ice nuclei properties within a Saharan dust event at the Jungfraujoch in the Swiss Alps, *Atmos. Chem. Phys.*, 11, 4725–4738, doi:10.5194/acp-11-4725-2011, 2011.
- Connolly, P. J., Möhler, O., Field, P. R., Saathoff, H., Burgess, R., Choulaton, T., and Gallagher, M.: Studies of heterogeneous freezing by three different desert dust samples, *Atmos. Chem. Phys.*, 9, 2805–2824, doi:10.5194/acp-9-2805-2009, 2009.
- Cziczo, D. J., Froyd, K. D., Hoose, C., Jensen, E. J., Diao, M. H., Zondlo, M. A., Smith, J. B., Twohy, C. H., and Murphy, D. M.: Clarifying the dominant sources and mechanisms of cirrus cloud formation, *Science*, 340, 1320–1324, 2013.
- DeMott, P. J., Sassen, K., Poellot, M. R., Baumgardner, D., Rogers, D. C., Brooks, S. D., Prenni, A. J., and Kreidenweis, S. M.: African dust aerosols as atmospheric ice nuclei, *Geophys. Res. Lett.*, 30, 1732, doi:10.1029/2003GL017410, 2003.

- DeMott, P. J., Prenni, A. J., Liu, X., Kreidenweis, S. M., Petters, M. D., Twohy, C. H., Richardson, M. S., Eidhammer, T., and Rogers, D. C.: Predicting global atmospheric ice nuclei distributions and their impacts on climate, *P. Natl. Acad. Sci. USA*, 107, 11217–11222, 2010.
- Duplissy, J., Enghoff, M. B., Aplin, K. L., Arnold, F., Aufmhoff, H., Avngaard, M., Baltensperger, U., Bondo, T., Bingham, R., Carslaw, K., Curtius, J., David, A., Fastrup, B., Gagné, S., Hahn, F., Harrison, R. G., Kellett, B., Kirkby, J., Kulmala, M., Laakso, L., Laaksonen, A., Lillestol, E., Lockwood, M., Mäkelä, J., Makhmutov, V., Marsh, N. D., Nieminen, T., Onnela, A., Pedersen, E., Pedersen, J. O. P., Polny, J., Reichl, U., Seinfeld, J. H., Sipilä, M., Stozhkov, Y., Stratmann, F., Svensmark, H., Svensmark, J., Veenhof, R., Verheggen, B., Viisanen, Y., Wagner, P. E., Wehrle, G., Weingartner, E., Wex, H., Wilhelmsson, M., and Winkler, P. M.: Results from the CERN pilot CLOUD experiment, *Atmos. Chem. Phys.*, 10, 1635–1647, doi:10.5194/acp-10-1635-2010, 2010.
- Duplissy, J., Merikanto, J., Franchin, A., Tsagkogeorgas, G., Kangasluoma, J., Wimmer, D., Vuollekoski, H., Schobesberger, S., Lehtipalo, K., Flagan, R. C., Brus, D., Donahue, N. M., Vehkamäki, H., Almeida, J., Amorim, A., Barmet, P., Bianchi, F., Breitenlechner, M., Dunne, E. M., Guida, R., Henschel, H., Junninen, H., Kirkby, J., Kürten, A., K., Määttänen, A., Makhmutov, V., Mathot, S., Nieminen, T., Onnela, A., Praplan, A. P., Riccobono, F., Rondo, L., Steiner, G., Tomé, A., Walther, H., Baltensperger, U., Carslaw, K. S., Dommen, J., Hansel, A., Petäjä, T., Sipilä, M., Stratmann, F., Virtanen, A., Wagner, P. E., Worsnop, D. R., Curtius, J., and Kulmala, M.: Effect of ions on sulfuric acid-water binary particle formation II: Experimental data and comparison with QC-normalized classical nucleation theory, *J. Geophys. Res.*, **in press**121, doi:10.1002/2015JD023539, **2015-2016**.
- Froyd, K. D., Murphy, D. M., Sanford, T. J., Thomson, D. S., Wilson, J. C., Pfister, L., and Lait, L.: Aerosol composition of the tropical upper troposphere, *Atmos. Chem. Phys.*, 9, 4363–4385, doi:10.5194/acp-9-4363-2009, 2009.
- Froyd, K. D., Murphy, D. M., Lawson, P., Baumgardner, D., and Herman, R. L.: Aerosols that form subvisible cirrus at the tropical tropopause, *Atmos. Chem. Phys.*, 10, 209–218, doi:10.5194/acp-10-209-2010, 2010.
- [Garimella, S., Kristensen, T. B., Ignatius, K., Welti, A., Voigtländer, J., Kulkarni, G. R., Sagan, F., Kok, G. L., Dorsey, J., Nichman, L., Rothenberg, D., Rösch, M., Kirchgäßner, A., Ladkin, R., Wex, H., Wilson, T. W., Ladino, L. A., Abbatt, J. P. D., Stetzer, O., Lohmann, U., Stratmann, F., and Cziczo, D. J.: The SPectrometer for Ice Nuclei \(SPIN\): An instrument to investigate ice nucleation, \*Atmos. Meas. Tech. Discuss.\*, doi:10.5194/amt-2015-400, \*\*in review\*\*, 2016.](#)

- Guenther, A., Hewitt, C. N., Erickson, D., Fall, R., Geron, C., Graedel, T., Harley, P., Klinger, L., Lerdau, M., Mckay, W. A., Pierce, T., Scholes, B., Steinbrecher, R., Tallamraju, R., Taylor, J., and Zimmerman, P.: A global model of natural volatile organic compound emissions, *J. Geophys. Res.-Atmos.*, 100, 8873–8892, 1995.
- Guenther, A., Karl, T., Harley, P., Wiedinmyer, C., Palmer, P. I., and Geron, C.: Estimates of global terrestrial isoprene emissions using MEGAN (Model of Emissions of Gases and Aerosols from Nature), *Atmos. Chem. Phys.*, 6, 3181–3210, doi:10.5194/acp-6-3181-2006, 2006.
- Hallquist, M., Wenger, J. C., Baltensperger, U., Rudich, Y., Simpson, D., Claeys, M., Dommen, J., Donahue, N. M., George, C., Goldstein, A. H., Hamilton, J. F., Herrmann, H., Hoffmann, T., Iinuma, Y., Jang, M., Jenkin, M. E., Jimenez, J. L., Kiendler-Scharr, A., Maenhaut, W., McFiggans, G., Mentel, Th. F., Monod, A., Prévôt, A. S. H., Seinfeld, J. H., Surratt, J. D., Szmigielski, R., and Wildt, J.: The formation, properties and impact of secondary organic aerosol: current and emerging issues, *Atmos. Chem. Phys.*, 9, 5155–5236, doi:10.5194/acp-9-5155-2009, 2009.
- Hoose, C. and Möhler, O.: Heterogeneous ice nucleation on atmospheric aerosols: a review of results from laboratory experiments, *Atmos. Chem. Phys.*, 12, 9817–9854, doi:10.5194/acp-12-9817-2012, 2012.
- Hoyle, C. R., Pinti, V., Welti, A., Zobrist, B., Marcolli, C., Luo, B., Höskuldsson, Á., Mattsson, H. B., Stetzer, O., Thorsteinsson, T., Larsen, G., and Peter, T.: Ice nucleation properties of volcanic ash from Eyjafjallajökull, *Atmos. Chem. Phys.*, 11, 9911–9926, doi:10.5194/acp-11-9911-2011, 2011.
- [Hoyle, C. R., Fuchs, C., Järvinen, E., Saathoff, H., Dias, A., El Haddad, I., Gysel, M., Coburn, S. C., Tröstl, J., Bernhammer, A.-K., Bianchi, F., Breitenlechner, M., Corbin, J. C., Craven, J., Donahue, N. M., Duplissy, J., Ehrhart, S., Frege, C., Gordon, H., Höppel, N., Heinritzi, M., Kristensen, T. B., Molteni, U., Nichman, L., Pinterich, T., Prévôt, A. S. H., Simon, M., Slowik, J. G., Steiner, G., Tomé, A., Vogel, A. L., Volkamer, R., Wagner, A. C., Wagner, R., Wexler, A. S., Williamson, C., Winkler, P. M., Yan, C., Amorim, A., Dommen, J., Curtius, J., Gallagher, M. W., Flagan, R. C., Hansel, A., Kirkby, J., Kulmala, M., Möhler, O., Stratmann, F., Worsnop, D. R., Baltensperger, U.: Aqueous phase oxidation of sulphur dioxide by ozone in cloud droplets, \*Atmos. Chem. Phys.\*, 16, 1693–1712, doi:10.5194/acp-16-1693-2016, 2016.](#)
- Ickes, L., Welti, A., Hoose, C., and Lohmann, U.: Classical nucleation theory of homogeneous freezing of water: thermodynamic and kinetic parameters, *Phys. Chem. Chem. Phys.*, 17, 5514–5537, 2015.
- Järvinen, E., Ignatius, K., Nichman, L., Kristensen, T. B., Fuchs, C., Höppel, N., Corbin, J. C., Craven, J., Duplissy, J., Ehrhart, S., El Haddad, I., Frege, C., Gates, S. J., Gordon, H., Hoyle, C. R.,

- Jokinen, T., Kallinger, P., Kirkby, J., Kiselev, A., Naumann, K.-H., Petäjä, T., Pinterich, T., Prevot, A. S. H., Saathoff, H., Schiebel, T., Sengupta, K., Simon, M., Tröstl, J., Virtanen, A., Vochezer, P., Vogt, S., Wagner, A. C., Wagner, R., Williamson, C., Winkler, P. M., Yan, C., Baltensperger, U., Donahue, N. M., Flagan, R. C., Gallagher, M., Hansel, A., Kulmala, M., Stratmann, F., Worsnop, D. R., Möhler, O., Leisner, T., and Schnaiter, M.: Observation of viscosity transition in  $\alpha$ -pinene secondary organic aerosol, *Atmos. Chem. Phys. Discuss.*, **15**, 28575–28617, doi: 2015-16, 3651–3664, 2016.
- Jimenez, J. L., Canagaratna, M. R., Donahue, N. M., Prevot, A. S. H., Zhang, Q., Kroll, J. H., DeCarlo, P. F., Allan, J. D., Coe, H., Ng, N. L., Aiken, A. C., Docherty, K. S., Ulbrich, I. M., Grieshop, A. P., Robinson, A. L., Duplissy, J., Smith, J. D., Wilson, K. R., Lanz, V. A., Hueglin, C., Sun, Y. L., Tian, J., Laaksonen, A., Raatikainen, T., Rautiainen, J., Vaattovaara, P., Ehn, M., Kulmala, M., Tomlinson, J. M., Collins, D. R., Cubison, M. J. E., Dunlea, J., Huffman, J. A., Onasch, T. B., Alfarra, M. R., Williams, P. I., Bower, K., Kondo, Y., Schneider, J., Drewnick, F., Borrmann, S., Weimer, S., Demerjian, K., Salcedo, D., Cottrell, L., Griffin, R., Takami, A., Miyoshi, T., Hatakeyama, S., Shimono, A., Sun, J. Y., Zhang, Y. M., Dzepina, K., Kimmel, J. R., Sueper, D., Jayne, J. T., Herndon, S. C., Trimborn, A. M., Williams, L. R., Wood, E. C., Middlebrook, A. M., Kolb, C. E., Baltensperger, U., and Worsnop, D. R.: Evolution of organic aerosols in the atmosphere, *Science*, **365**, 1525–1529, 2009.
- Kanakidou, M., Seinfeld, J. H., Pandis, S. N., Barnes, I., Dentener, F. J., Facchini, M. C., Van Dingenen, R., Ervens, B., Nenes, A., Nielsen, C. J., Swietlicki, E., Putaud, J. P., Balkanski, Y., Fuzzi, S., Horth, J., Moortgat, G. K., Winterhalter, R., Myhre, C. E. L., Tsigaridis, K., Vignati, E., Stephanou, E. G., and Wilson, J.: Organic aerosol and global climate modelling: a review, *Atmos. Chem. Phys.*, **5**, 1053–1123, doi:10.5194/acp-5-1053-2005, 2005.
- Kirkby, J., Curtius, J., Almeida, J., Dunne, E., Duplissy, J., Ehrhart, S., Franchin, A., Gagne, S., Ickes, L., Kürten, A., Kupc, A., Metzger, A., Riccobono, F., Rondo, L., Schobesberger, S., Tsigakgeorgas, G., Wimmer, D., Amorim, A., Bianchi, F., Breitenlechner, M., David, A., Dommen, J., Downard, A., Ehn, M., Flagan, R. C., Haider, S., Hansel, A., Hauser, D., Jud, W., Junninen, H., Kreissl, F., Kvashin, A., Laaksonen, A., Lehtipalo, K., Lima, J., Lovejoy, E. R., Makhmutov, V., Mathot, S., Mikkilä, J., Minginette, P., Mogo, S., Nieminen, T., Onnela, A., Pereira, P., Petäjä, T., Schnitzhofer, R., Seinfeld, J. H., Sipilä, M., Stozhkov, Y., Stratmann, F., Tomé, A., Vanhanen, J., Viisanen, Y., Vrtala, A., Wagner, P. E., Walther, H., Weingartner, E., Wex, H., Winkler, P. M., Carslaw, K. E., Worsnop, D. R., Baltensperger, U., and Kulmala, M.: Role of sulphuric acid, ammonia and galactic cosmic rays in atmospheric aerosol nucleation, *Nature*, **476**, 429–433, 2011.

- Koop, T., Luo, B., Tsias, A., and Peter, T.: Water activity as the determinant for homogeneous ice nucleation in aqueous solutions, *Nature*, 406, 611–614, 2000.
- Koop, T., Bookhold, J., Shiraiwa, M., and Pöschl, U.: Glass transition and phase state of organic compounds: dependency on molecular properties and implications for secondary organic aerosols in the atmosphere, *Phys. Chem. Chem. Phys.*, 13, 19238–19255, 2011.
- Krämer, M., Schiller, C., Afchine, A., Bauer, R., Gensch, I., Mangold, A., Schlicht, S., Spelten, N., Sitnikov, N., Borrmann, S., de Reus, M., and Spichtinger, P.: Ice supersaturations and cirrus cloud crystal numbers, *Atmos. Chem. Phys.*, 9, 3505–3522, doi:10.5194/acp-9-3505-2009, 2009.
- Kulmala, M., Laaksonen, A., and Pirjola, L.: Parameterizations for sulfuric acid/water nucleation rates, *J. Geophys. Res.*, 103, 8301–8307, 1998.
- Laaksonen, A., Kulmala, M., O'Dowd, C. D., Joutsensaari, J., Vaattovaara, P., Mikkonen, S., Lehtinen, K. E. J., Sogacheva, L., Dal Maso, M., Aalto, P., Petäjä, T., Sogachev, A., Yoon, Y. J., Lihavainen, H., Nilsson, D., Facchini, M. C., Cavalli, F., Fuzzi, S., Hoffmann, T., Arnold, F., Hanke, M., Sellegri, K., Umann, B., Junkermann, W., Coe, H., Allan, J. D., Alfarra, M. R., Worsnop, D. R., Riekkola, M.-L., Hyötyläinen, T., and Viisanen, Y.: The role of VOC oxidation products in continental new particle formation, *Atmos. Chem. Phys.*, 8, 2657–2665, doi:10.5194/acp-8-2657-2008, 2008.
- Ladino, L. A., Zhou, S., Yakobi-Hancock, J. D., Aljawhary, D., and Abbatt, J. P. D.: Factors controlling the ice nucleating abilities of  $\alpha$ -pinene SOA particles, *J. Geophys. Res.-Atmos.*, 119, 9041–9051, 2014.
- [Lienhard, D. M., Huisman, A. J., Krieger, U. K., Rudich, Y., Marcolli, C., Luo, B. P., Bones, D. L., Reid, J. P., Lambe, A. T., Ganagaratna, M. R., Davidovits, P., Onasch, T. B., Worsnop, D. R., Steimer, S. S., Koop, T. and Peter, T.: Viscous organic aerosol particles in the upper troposphere: diffusivity-controlled water uptake and ice nucleation?, \*Atmos. Chem. Phys.\*, 15, 13599–13613, 2015.](#)
- Mann, G. W., Carslaw, K. S., Spracklen, D. V., Ridley, D. A., Manktelow, P. T., Chipperfield, M. P., Pickering, S. J., and Johnson, C. E.: Description and evaluation of GLOMAP-mode: a modal global aerosol microphysics model for the UKCA composition-climate model, *Geosci. Model Dev.*, 3, 519–551, doi:10.5194/gmd-3-519-2010, 2010.
- Möhler, O., Field, P. R., Connolly, P., Benz, S., Saathoff, H., Schnaiter, M., Wagner, R., Cotton, R., Krämer, M., Mangold, A., and Heymsfield, A. J.: Efficiency of the deposition mode ice nucleation on mineral dust particles, *Atmos. Chem. Phys.*, 6, 3007–3021, doi:10.5194/acp-6-3007-2006, 2006.

- Möhler, O., Benz, S., Saathoff, H., Schnaiter, M., Wagner, R., Schneider, J., Walter, S., Ebert, V., and Wagner, S.: The effect of organic coating on the heterogeneous ice nucleation efficiency of mineral dust aerosols, *Env. Res. Lett.*, 3, 025007, doi:10.1088/1748-9326/3/2/025007, 2008.
- Murray, B. J., Wilson, T. W., Dobbie, S., Cui, Z., Al-Jumur, S. M., Möhler, O., Schnaiter, M., Wagner, R., Benz, S., Niemand, M., Saathoff, H., Ebert, V., Wagner, S., and Kärcher, B.: Heterogeneous nucleation of ice particles on glassy aerosols under cirrus conditions, *Nat. Geosci.*, 3, 233–237, 2010.
- [Murray, B. J., O'Sullivan, D., Atkinson, J. D. and Webb, M. E. : Ice nucleation by particles immersed in supercooled cloud droplets, \*Chem. Soc. Rev.\*, 41, 6519–6554, 2012.](#)
- Nichman, L., Fuchs, C., Järvinen, E., Ignatius, K., Höppel, N. F., Dias, A., Heinritzi, M., Simon, M., Tröstl, J., Wagner, A. C., Wagner, R., Williamson, C., Yan, C., Bianchi, F., Connolly, P. J., Dorsey, J. R., Duplissy, J., Ehrhart, S., Frege, C., Gordon, H., Hoyle, C. R., Kristensen, T. B., Steiner, G., Donahue, N. M., Flagan, R., Gallagher, M. W., Kirkby, J., Möhler, O., Saathoff, H., Schnaiter, M., Stratmann, F., and Tomé, A.: Discrimination of water, ice and aerosols by light polarisation in the CLOUD experiment, *Atmos. Chem. Phys. Discuss.*, 15, 31433–31469, 2015. [16, 3651–3664, 2016.](#)
- Pajunoja, A., Lambe, A. T., Hakala, J., Rastak, N., Cummings, M. J., Brogan, J. F., Hao, L., Paramonov, M., Hong, J., Prisle, N. L., Malila, J., Romakkaniemi, S., Lehtinen, K. E. J., Laaksonen, A., Kulmala, M., Massoli, P., Onasch, T. B., Donahue, N. M., Riipinen, I., Davidovits, P., Worsnop, D., Petäjä, T., and Virtanen, A.: Adsorptive uptake of water by semisolid secondary organic aerosols, *Geophys. Res. Lett.*, 42, 3063–3068, 2015.
- [Price, H. C., Mattsson, J., Zhang, Y., Bertram, A. K., Davies, J. F., Grayson, J. W., Martin, S. T., O'Sullivan, D., Reid, J. P., Rickards, A. M. J., and Murray, B. J.: Water diffusion in atmospherically relevant  \$\alpha\$ -pinene secondary organic material, \*Chem. Sci.\*, 6, 4876–4883, 2015.](#)
- Pruppacher, H. R. and Klett, J. D.: *Microphysics of Clouds and Precipitation*, Atmospheric and Oceanographic Sciences Library, Kluwer Academic Publishers, Dordrecht, the Netherlands, 1997.
- [Pummer, B. G., Bauer, H., Bernardi, J., Bleicher, S., and Grothe, H.: Suspendable macromolecules are responsible for ice nucleation activity of birch and conifer pollen, \*Atmos. Chem. Phys.\*, 12, 2541–2550, 2012.](#)
- Renbaum-Wolff, L., Grayson, J., Bateman, A. P., Kuwata, K., Sellier, M., Murray, B. J., Schilling, J. E., Martin, S. T., and Bertram, A. K.: Viscosity of  $\alpha$ -pinene secondary organic material and implications for particle growth and reactivity, *P. Natl. Acad. Sci. USA*, 110, 8014–8019, 2013.

- Riccobono, F., Schobesberger, S., Scott, C. E., Dommen, J., Ortega, I. K., Rondo, L., Almeida, J., Amorim, A., Bianchi, F., Breitenlechner, M., David, A., Downard, A., Dunne, E. M., Duplissy, J., Ehrhart, S., Flagan, R. C., Franchin, A., Hansel, A., Junninen, H., Kajos, M., Keskinen, H., Kupc, A., Kürten, A., Kvashin, A. N., Laaksonen, A., Lehtipalo, K., Makhmutov, V., Mathot, S., Nieminen, T., Onnela, A., Petäjä, T., Praplan, A. P., Santos, F. D., Schallhart, S., Seinfeld, J. H., Sipilä, M., Spracklen, D. V., Stozhkov, Y., Stratmann, F., Tomé, A., Tsagkogeorgas, G., Vaattovaara, P., Viisanen, Y., Virtala, A., Wagner, P. E., Weingartner, E., Wex, H., Wimmer, D., Carslaw, K. S., Curtius, J., Donahue, N. M., Kirkby, J., Kulmala, M., Worsnop, D. R., and Baltensperger, U.: Oxidation products of biogenic emissions contribute to nucleation of atmospheric particles, *Science*, 344, 717–721, 2014.
- Rogers, D. C.: Development of a continuous flow thermal gradient diffusion chamber for ice nucleation studies, *Atmos. Res.*, 22, 149–181, 1988.
- Schill, G. P., De Haan, D. O., and Tolbert, M. A.: Heterogeneous ice nucleation on simulated secondary organic aerosol, *Environ. Sci. Technol.*, 48, 1675–1682, 2014.
- Seinfeld, J. H. and Pandis, S. N.: *Atmospheric Chemistry and Physics: From Air Pollution to Climate Change*, 2nd edn., John Wiley and Sons, Inc., Hoboken, New Jersey, USA, 2006.
- Stetzer, O., Baschek, B., Lüönd, F., and Lohmann, U.: The Zurich Ice Nucleation Chamber (ZINC) – a new instrument to investigate atmospheric ice formation, *Aerosol Sci. Tech.*, 42, 64–72, 2008.
- Suni, T., Hakola, H., Bäck, J., Hurley, R., van Gorsel, E., Ruuskanen, T., Kulmala, M., Sogacheva, L., Leuning, R., Cleugh, H., and Keith, H.: Effect of vegetation on aerosol formation in South-East Australia, in: *Nucleation and Atmospheric Aerosols*, edited by: O’Dowd, C. D. and Wagner, P. E., Springer Netherlands, 1018–1022, 2007.
- Virtanen, A., Joutsensaari, J., Koop, T., Kannosto, J., Ylipirilä, P., Leskinen, J., Mäkelä, J. M., Holopainen, J. K., Pöschl, U., Kulmala, M., Worsnop, D. R., and Laaksonen, A.: An amorphous solid state of biogenic secondary organic aerosol particles, *Nature*, 467, 824–827, 2010.
- Wagner, R., Möhler, O., Saathoff, H., Schnaiter, M., Skrotzki, J., Leisner, T., Wilson, T. W., Malkin, T. L., and Murray, B. J.: Ice cloud processing of ultra-viscous/glassy aerosol particles leads to enhanced ice nucleation ability, *Atmos. Chem. Phys.*, 12, 8589–8610, doi:10.5194/acp-12-8589-2012, 2012.
- Wang, B., Lambe, A. T., Massoli, P., Onasch, T. B., Davidovitch, P., Worsnop, D. R., and Knopf, D. A.: The deposition ice nucleation and immersion freezing potential of amorphous secondary organic aerosol: pathways for ice and mixed-phase cloud formation, *J. Geophys. Res.-Atmos.*, 117, D16209, doi:10.1029/2012JD018063, 2012.

- Welti, A., Lüönd, F., Stetzer, O., and Lohmann, U.: Influence of particle size on the ice nucleating ability of mineral dusts, *Atmos. Chem. Phys.*, 9, 6705–6715, doi:10.5194/acp-9-6705-2009, 2009.
- ~~Wilcoxon, F.: Individual comparisons by ranking methods, *Biometrics Bull.*, 1, 80–83, 1945.~~
- Wilson, T. W., Murray, B. J., Wagner, R., Möhler, O., Saathoff, H., Schnaiter, M., Skrotzki, J., Price, H. C., Malkin, T. L., Dobbie, S., and Al-Jumur, S. M. R. K.: Glassy aerosols with a range of compositions nucleate ice heterogeneously at cirrus temperatures, *Atmos. Chem. Phys.*, 12, 8611–8632, doi:10.5194/acp-12-8611-2012, 2012.
- Wu, Z. J., Nowak, A., Poulain, L., Herrmann, H., and Wiedensohler, A.: Hygroscopic behavior of atmospherically relevant water-soluble carboxylic salts and their influence on the water uptake of ammonium sulfate, *Atmos. Chem. Phys.*, 11, 12617–12626, doi:10.5194/acp-11-12617-2011, 2011.
- Yu, H., Kaufman, Y. J., Chin, M., Feingold, G., Remer, L. A., Anderson, T. L., Balkanski, Y., Belouin, N., Boucher, O., Christopher, S., DeCola, P., Kahn, R., Koch, D., Loeb, N., Reddy, M. S., Schulz, M., Takemura, T., and Zhou, M.: A review of measurement-based assessments of the aerosol direct radiative effect and forcing, *Atmos. Chem. Phys.*, 6, 613–666, doi:10.5194/acp-6-613-2006, 2006.
- Zobrist, B., Marcolli, C., Pedernera, D. A., and Koop, T.: Do atmospheric aerosols form glasses?, *Atmos. Chem. Phys.*, 8, 5221–5244, doi:10.5194/acp-8-5221-2008, 2008.

**Table 1.** The conditions for the ice nucleation experiments with viscous  $\alpha$ -pinene SOA. The columns from left to right list the dates when the experiment was carried out, the average temperature in the CLOUD chamber during the particle sampling with the ~~IN~~-INP counter SPIN, the average relative humidity with respect to water  $RH_w$  in the CLOUD chamber, mean particle mobility diameters and the sampled particle number concentrations measured by the SPIN optical particle counter (OPC) and a Condensation Particle Counter (CPC). For each experiment, 1 to 4 ice nucleation onset measurements were performed. The CPC was operated parallel to SPIN during half of the runs. For the runs without CPC number concentrations, frozen fractions could be estimated from the SPIN OPC particle number concentrations and size distributions.

Date	Chamber $T$ ( $^{\circ}\text{C}$ )	Chamber $RH_w$ (%)	Particle diameter (nm)	SPIN OPC conc. ( $\text{cm}^{-3}$ )	CPC conc. ( $\text{cm}^{-3}$ )
25 Oct	-10	12	800	200	-
26 Oct	-20	10	550, 600	150-600	-
27 Oct	-20	10	800	150	150
28 Oct	-30	10	320, 630	-	490
29 Oct	-38	10	330	-	310
3 Nov	-38	60	120	-	130

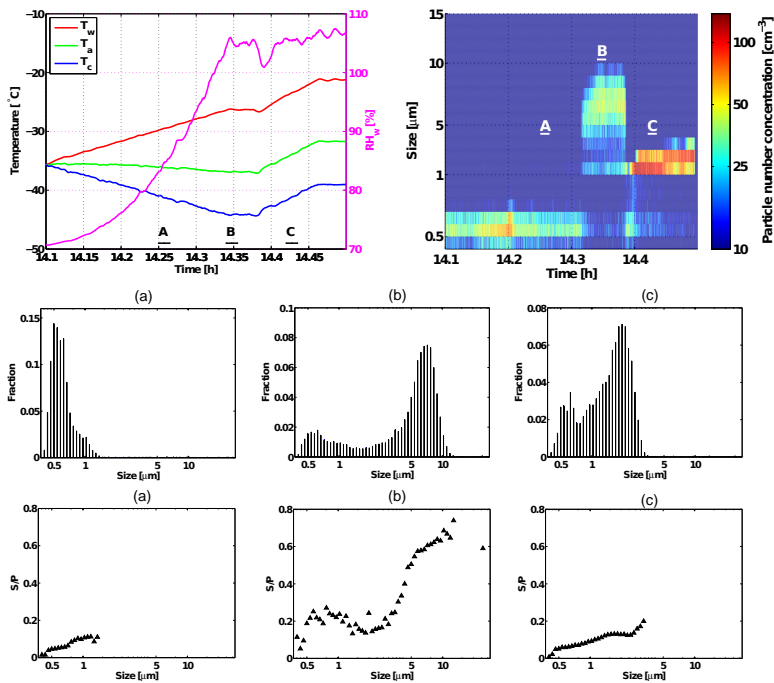


**Figure 1.** Homogeneous freezing of highly diluted ammonium sulphate droplets. In the top left panel, the SPIN cold and warm wall ( $T_c$  and  $T_w$ ) and sample (lamina) temperatures ( $T_a$ ), as well as the relative humidity with respect to liquid water ( $RH_w$ ) are plotted as a function of time. The top right panel shows the particle number concentrations in different size bins from the same experiment. Bars A, B, C in the top panels mark the time intervals from which the normalised SPIN OPC particle number size distributions and the median values of the polarisation-equivalent  $S/P$  ratios are shown in the corresponding lower panels. In (a) seed particles, in (b) seed and ice particles, in (c) seed particles and liquid droplets. The size distributions and  $S/P$  ratios are averaged over 54 s, and correspond to the following times in the upper panels: (a) 14.25–14.265 h, (b) 14.34–14.355 h, (c) 14.42–14.435 h.

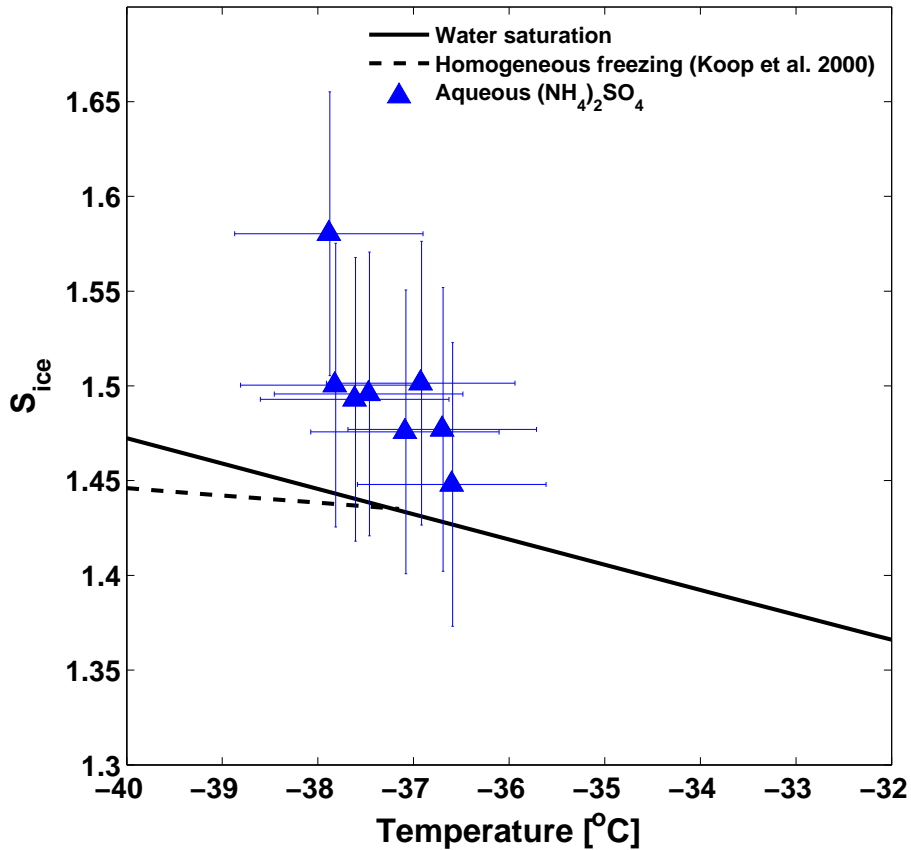


**Figure 2.** Homogeneous freezing temperatures of highly diluted ammonium sulphate droplets measured with SPIN. The frozen fraction here is 10%. The uncertainties in temperature and ice saturation ratio shown here correspond to the 95% confidence interval calculated from the statistical standard deviation. The homogeneous freezing line from Koop et al. (2000) is calculated for 500 nm particles.

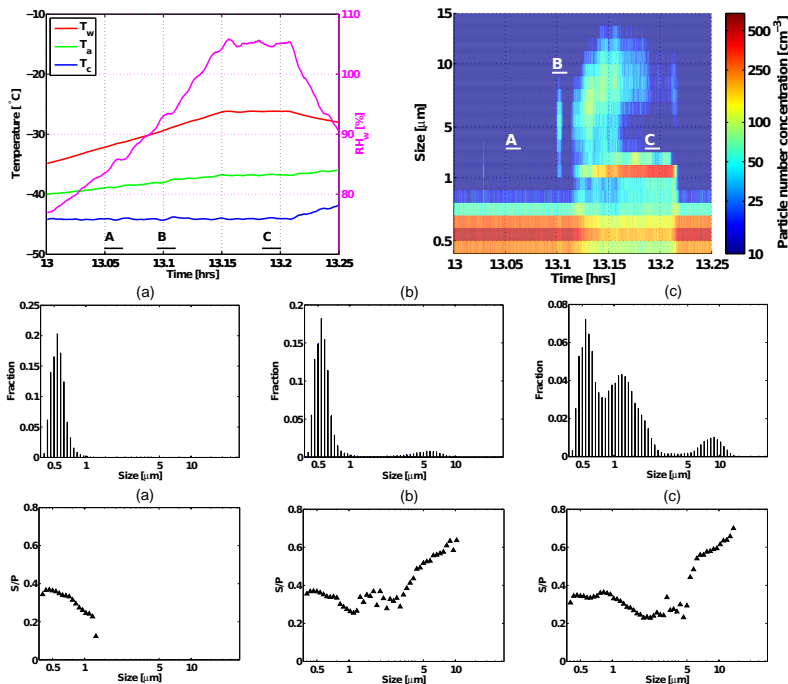


**Figure 3.** Deposition-Heterogeneous ice nucleation of viscous  $\alpha$ -pinene SOA particles from 26.10.2014. Analogously to Fig. 1, the top left panel shows the SPIN wall and lamina temperatures and the  $RH_w$  as a function of time, and the top right panel the particle number concentrations in different size bins. Also here, bars A, B, C in the upper panels correspond to the time intervals from which the normalised SPIN OPC particle number size distributions and median values of polarisation-equivalent  $S/P$  ratios are shown in the lower panels. Panel (a) shows the 550 nm seed aerosol and panel (b) depicts seeds and ice crystals at water subsaturated conditions. A prominent liquid (frozen) droplet mode can be seen in panel (c), when homogeneous-freezing was observed at water supersaturation. The size distributions are averaged over 54 s and correspond to the following times in the upper panels: (a) 13.05–13.065 h, (b) 13.095–13.11 h, (c) 13.185–13.2 h.

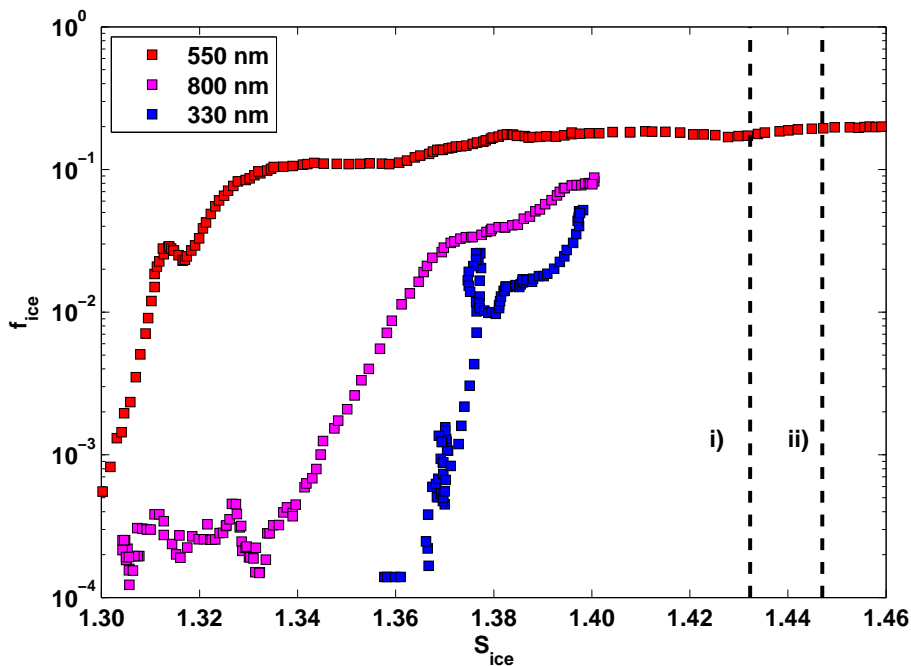


**Figure 4.** Examples of frozen fractions of viscous  $\alpha$ -pinene SOA obtained with SPIN as a function of the ice saturation ratio  $S_{ice}$ . The blue squares correspond to seed aerosol of 330 nm, formed at  $-38^{\circ}\text{C}$ , the red squares are the 550 nm particles, formed at  $-20^{\circ}\text{C}$ , and the magenta squares are 800 nm particles, formed at  $-10^{\circ}\text{C}$ . At the time of ice formation, the aerosol sample temperature inside SPIN was kept at approximately  $-37.7$ – $38.5^{\circ}\text{C}$  for 330 nm particles; for 550 nm particles the temperature was at  $-38.1$ – $37.2^{\circ}\text{C}$  and for 800 nm particles at  $-37.0$ – $38.2^{\circ}\text{C}$ . The black dashed vertical lines correspond to water saturation at (i)  $-37^{\circ}\text{C}$  and (ii)  $-38^{\circ}\text{C}$ . Ice activation thresholds (1, 0.15, 10%) were determined from similar ice activation graphs.

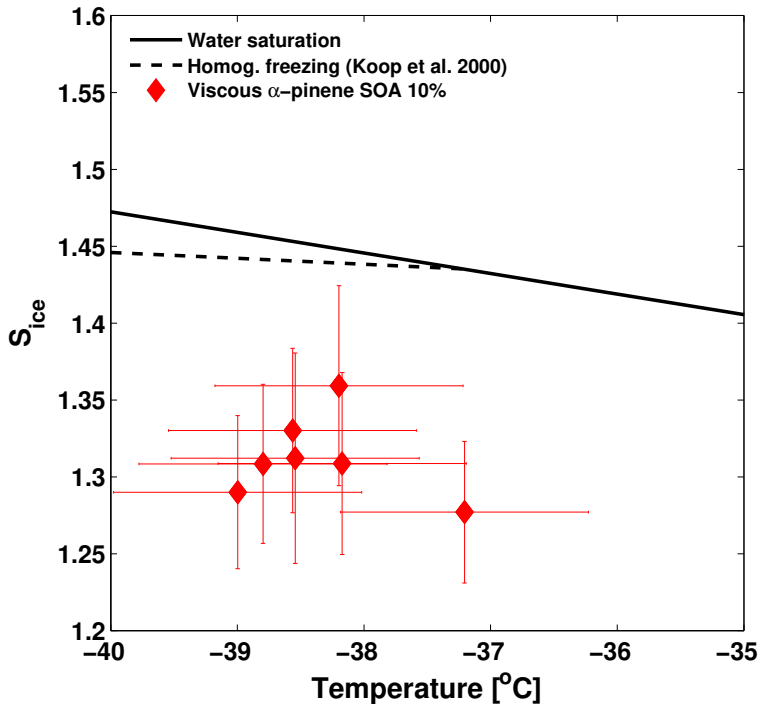


**Figure 5.** Ice nucleation onsets ( $\pm 10\%$  activation) for  $\alpha$ -pinene SOA in the deposition (red diamonds) and homogeneous (cyan diamond) freezing mode. The horizontal error bars of the deposition ice nucleation data represent statistical 95 % confidence interval in both temperature and supersaturation, and are calculated from the instrumentally determined standard deviation. Homogeneous freezing onset was observed only once, hence of  $0.5^\circ\text{C}$  in the homogeneous freezing experiments. The error bars in supersaturation correspond to ice saturation ratio illustrate the theoretical modelled maximum error calculated from equilibrium range the estimated instrumental temperature uncertainty aerosol sample can be exposed to.

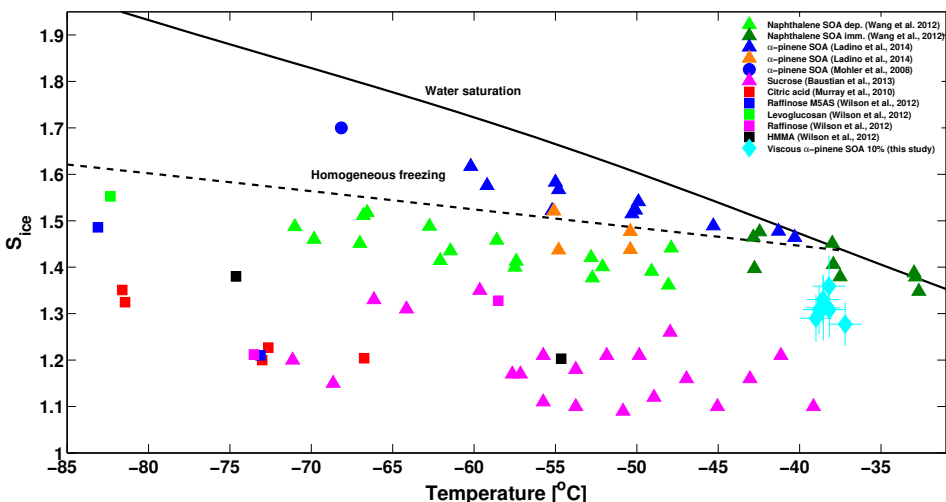


**Figure 6.** Comparison of ice nucleation onsets of different SOA species and proxies. The black solid line is the water saturation line and the black dashed line the Koop et al. (2000) homogeneous freezing line for 500 nm particles. The red and cyan diamonds represent the results of this study; the light and dark green triangles deposition nucleation and immersion freezing of naphthalene SOA from Wang et al. (2012); the magenta triangles deposition ice nucleation of sucrose from Baustian et al. (2013); the blue triangles ice nucleation of  $\alpha$ -pinene SOA studied by Ladino et al. (2014) and the orange triangles pre-cooled  $\alpha$ -pinene SOA from the same study; and the blue circle depicts the homogeneous freezing of pure  $\alpha$ -pinene SOA reported by Möhler et al. (2008). The red squares show the deposition ice nucleation onsets for glassy citric acid (Murray et al., 2010), and the freezing results of 4 glassy SOA proxies from Wilson et al. (2012) are shown by blue squares (raffinose M5AS), green squares (levoglucosan), magenta squares (raffinose), and black squares (HMMAs).

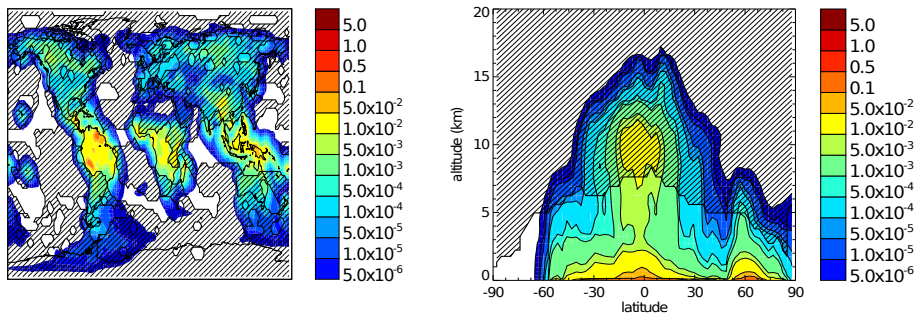


**Figure 7.** GLOMAP model predictions of mean annual concentrations of condensable oxidation products of monoterpenes, SORG. The concentrations shown by the colourscale are in parts per trillion with respect to mass (pptm). The hatched areas represent the zones where the SOA particles could exist in a highly viscous or amorphous phase state in the upper troposphere and potentially affect cirrus cloud formation through [deposition](#) ice nucleation [or immersion freezing](#). The calculations for these zones are based on the theoretical estimate of generic SOA glass transition temperature as a function of relative humidity presented by Koop et al. (2011). The left panel shows a global map of the mean annual concentrations of SORG at a sigma-pressure level corresponding to approximately 6900 m altitude from a simulation of the year 2000. In the right panel, annual zonal mean of global concentrations of SORG are plotted as a function of latitude and altitude.

**Supplementary information to  
"Heterogeneous ice nucleation of viscous secondary organic aerosol  
produced from ozonolysis of  $\alpha$ -pinene"**

K. Ignatius et al.

*Correspondence to:* Karoliina Ignatius (ignatius@tropos.de)

**Table S1.** The viscous  $\alpha$ -pinene SOA ice nucleation onset conditions for frozen fractions of 1 %, 5 % and 10 %. The columns from left to right list the date and the SPIN experiment number, the frozen (activated) fraction  $f_{ice}$ , the ice nucleation onset temperature, the minimum modelled saturation ratio with respect to water in SPIN ( $S_w$  min), the maximum modelled saturation ratio with respect to water in SPIN ( $S_w$  max), the minimum modelled saturation ratio with respect to ice in SPIN ( $S_{ice}$  min), and the maximum modelled saturation ratio with respect to ice in SPIN ( $S_{ice}$  max).

Date, Exp	$f_{ice}$ (%)	Temperature ( $^{\circ}$ C)	$S_w$ min	$S_w$ max	$S_{ice}$ min	$S_{ice}$ max
25 Oct, 1	1	-38.2	0.87	0.95	1.26	1.38
25 Oct, 1	5	-38.3	0.88	0.97	1.27	1.40
25 Oct, 1	10	-38.2	0.89	0.98	1.29	1.42
26 Oct, 1	1	-39.0	0.85	0.91	1.24	1.33
26 Oct, 1	5	-39.0	0.85	0.91	1.24	1.33
26 Oct, 1	10	-39.0	0.85	0.92	1.24	1.34
26 Oct, 2	1	-38.8	0.85	0.92	1.24	1.34
26 Oct, 2	5	-38.8	0.86	0.93	1.25	1.35
26 Oct, 2	10	-38.8	0.86	0.93	1.26	1.36
26 Oct, 3	1	-37.2	0.86	0.91	1.23	1.31
26 Oct, 3	5	-37.2	0.86	0.92	1.23	1.32
26 Oct, 3	10	-37.2	0.86	0.92	1.23	1.32
27 Oct, 1	1	-38.1	0.86	0.93	1.24	1.35
27 Oct, 1	5	-38.1	0.86	0.94	1.25	1.36
27 Oct, 1	10	-38.2	0.86	0.94	1.25	1.37
28 Oct, 1	1	-39.0	0.84	0.90	1.23	1.31
28 Oct, 1	5	-38.5	0.85	0.95	1.23	1.39
28 Oct, 1	10	-38.5	0.86	0.95	1.24	1.38
28 Oct, 2	1	-38.7	0.87	0.95	1.26	1.38
28 Oct, 2	5	-38.6	0.88	0.95	1.27	1.38
28 Oct, 2	10	-38.6	0.88	0.95	1.28	1.38
29 Oct, 1	1	-38.5	0.89	0.98	1.29	1.42
29 Oct, 1	5	-38.5	0.89	0.98	1.29	1.42
29 Oct, 1	10	-	-	-	-	-

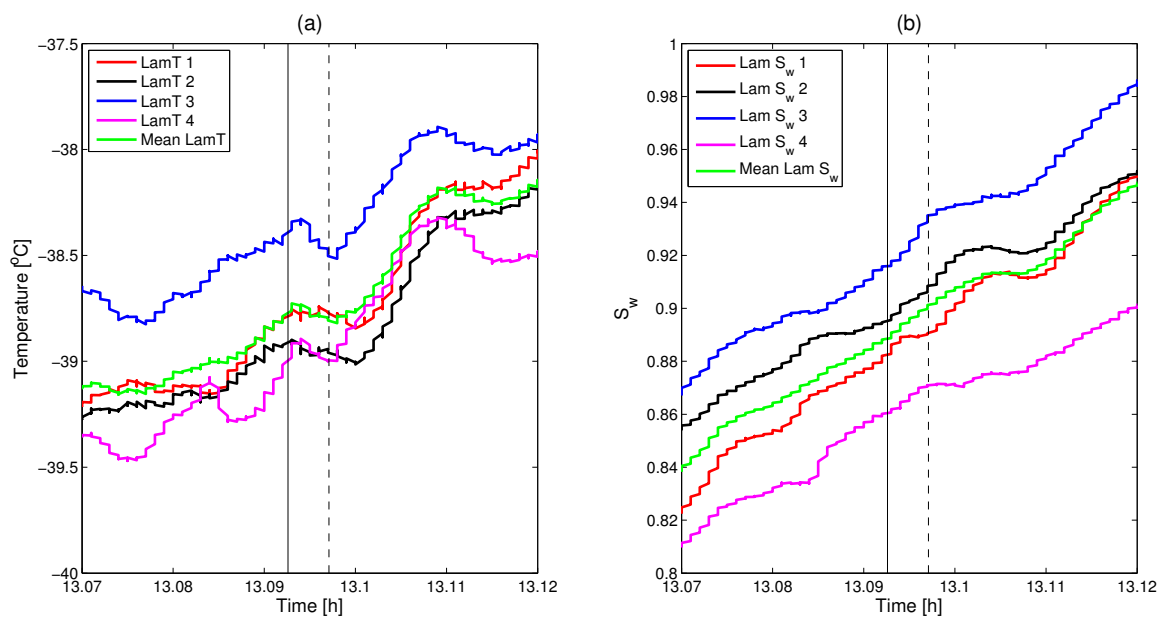


**Figure S1.** Aerosol lamina temperatures and maximum modelled water saturation ratios ( $S_w$ ) during the ice nucleation onset of 550 nm SOA particles depicted in Fig. 3. In panel (a), the aerosol lamina temperatures at 4 locations inside SPIN are plotted. The lamina temperatures are calculated according to the modelling of the buoyancy effect by Rogers (1988), from the temperature readings monitored at 4 thermocouple locations on the SPIN chamber walls. The numbers 1 to 4 denote the different thermocouple locations. The mean lamina temperature is the mean of the 4 depicted lamina temperatures. In panel (b), the calculated lamina saturation ratios with respect to water at the 4 thermocouple locations are shown, as well as their mean. The black solid and dashed vertical lines depict the observed 1 % and 10 % ice activation thresholds, respectively. The maximum modelled  $S_w$  range for each ice nucleation onset is the range between the highest and the lowest lamina  $S_w$ .

## References

Rogers, D. C.: Development of a continuous flow thermal gradient diffusion chamber for ice nucleation studies, *Atmos. Res.*, 22, 149–181, 1988.